Research on Engineering Structures & Materials
www.jresm.org
Research Group

Research Article

Experimental evaluation of high-performance recycled aggregate concrete enhanced with calcined kaolin clay and alkali-resistant glass fibres

Olutosin Peter Akintunde [*,1,2,a], Jacques Snyman [1,b], Chris Ackerman [1,c], Williams K. Kupolati [1,d]

[1]*Department of Civil Engineering, Faculty of Engineering and the Built Environment, Tshwane University of Technology, Pretoria 0001, South Africa*
[2]*Department of Civil Engineering, Faculty of Technology, University of Ibadan, Ibadan, Nigeria*

Article Info

Article History:

Received 06 Oct 2025
Accepted 11 May 2026

Keywords:

High-performance recycled;
Aggregate concrete;
Calcined kaolin clay;
Alkali resistant glass fibre;
Superplasticizers;
Experimental investigation;
Mechanical and durability properties

Abstract

At high replacement levels, recycled aggregate concrete (RAC) has durability consequences because of its porosity and weak interfacial transition zones (ITZs). This study examines how alkali-resistant glass fiber (ARGF) and calcined kaolin clay (CKC) work together to produce high-performance RAC (HP-RAC). Recycled coarse aggregate (RCA: 0–100%), CKC (0–15% by mass), and ARGF (0–1.5% by mass of concrete) were used in a full factorial design with a constant low water–binder ratio of 0.37. The freshness, mechanical qualities, and durability up to 91 days of 80 mixtures were assessed. According to the results, ARGF increased tensile and flexural performance through crack-bridging without compromising transport characteristics, whereas CKC reduced sorptivity, chloride ingress, and sulphate damage while also significantly improving matrix densification. Performance was negatively impacted by RCA replacement above 50%, although liabilities were lessened at about 25% replacement when 10–15% CKC and 0.5% ARGF were added, resulting in compressive strengths above 60 MPa and compliance with protective durability classes. With substantial RCA×CKC interactions, statistical analysis (ANOVA, R2 = 0.977, $p < 0.0001$) validated the importance of mix design parameters. The results show that ARGF is a serviceability modifier and CKC is the main durability lever in HP-RAC, providing a verified route for sustainable structural concrete made from demolition waste.

1. Introduction

In light of its importance to infrastructure, concrete is essential but challenging to decarbonize. The cement subsector is still "not on track" for the Net Zero pathway because direct CO_2 intensity reductions since 2015 have been limited, and significant near-term mitigation still depends on material efficiency, clinker substitution, and the implementation of the Crushed Cement Utilization Strategy by 2030. According to the IEA's 2023–2024 projections, efficiency gains in some locations have been countered by greater clinker-to-cement ratios, however overall sector emissions must decrease by about 20% by 2030 [1]. Due to these system-level limitations, mix design levers—specifically, circular aggregates and supplemental cementitious materials (SCMs)—that can be used immediately to lessen embodied impacts without compromising performance are crucial [2].

Recycled aggregate concrete (RAC), which keeps natural aggregates from going to landfills and diverts construction and demolition waste (C&DW), presents a significant potential. Recent

*Corresponding author: AkintundeOP@tut.ac.za
[a]orcid.org/0000-0002-6523-9210; [b]orcid.org/ 0000-0003-2309-4153; [c]orcid.org/ 0009-0007-3162-3496; [d]orcid.org/ 0000-0002-2574-2671
DOI: http://dx.doi.org/10.17515/resm2026-1217ma1006rs

reviews and experimental syntheses (2023–2025) demonstrate that, with proper mixture design and conditioning, RAC can achieve competitive mechanical performance in structural applications; however, workability, stiffness, and transport properties are still challenged by RCA's higher porosity and water absorption. Meta inferences from recent datasets, in particular, agree on a strong performance window of about 20–30% RCA (by mass of coarse aggregate) for conventional designs. Higher replacement levels are possible in performance-engineered systems that incorporate micro reinforcement, high range water reducers, and SCMs [3,4].

In order to attain high strength classes (such as C50/60) and greater durability (low permeability, enhanced chemical resistance), High Performance Recycled Aggregate Concrete (HPRAC) expands on RAC by using fibers, SCMs, and low water-binder ratios (w/b) [5]. According to recent research, the interfacial transition zone (ITZ) surrounding RCA and the mortar to which it is bonded controls a number of property deficiencies, including porosity, water absorption, and chloride transport. For this reason, reactive SCMs are required to stabilize the ITZ and improve pore networks. Conversely, discrete fibers can improve tensile/flexural performance and post-cracking toughness in low w/b matrices without impairing transport when dosed carefully [6-8].

Despite the inherent variability of recycled coarse aggregates, High Performance Recycled Aggregate Concrete (HP RAC) is an advancement of traditional recycled aggregate concrete that aims to achieve high strength, low permeability, and better durability. Low water-binder ratios, reactive supplemental cementitious ingredients, and sophisticated admixture technology—often enhanced by discrete fibers—all contribute to its performance. By strengthening the interfacial transition zone, controlling crack propagation, and refining the pore structure, these actions allow HP RAC to satisfy the endurance and structural requirements for harsh environments [9].

A highly reactive Class F pozzolan, calcined kaolin clay (metakaolin, herein CKC) is particularly appealing among SCMs because it consumes portlandite and aids in the development of C (A) S H, which improves pore refinement and resistance to chloride ingress [10,11]. However, it has a well-known trade-off of increased water demand, which can be compensated for by contemporary polycarboxylate superplasticizers. Its durability and strength advantages are confirmed by thorough evaluations and performance studies (2020–2025) for a variety of concretes, including high performance systems. (Updated industry guidelines and research papers confirm metakaolin's present significance as a pivotal supply chain management (SCM) for performance engineering, even though many classic studies precede 2020 [12].

Kaolinitic clay is heated to 600–800 °C to create calcined kaolin clay, also known as metakaolin, a highly reactive aluminosilicate. The clay is dehydroxylated by this thermal activation, resulting in an amorphous phase with potent pozzolanic activity. CKC densifies the matrix, improves pore structure, and decreases capillary connectivity in cementitious systems by reacting with calcium hydroxide that is produced during hydration to create more calcium silicate and aluminosilicate hydrates [13]. By strengthening the interfacial transition zone and decreasing permeability, CKC increases the compressive and tensile strength of high-performance concrete, especially at later ages. By reducing chloride infiltration and boosting resistance to sulphate assault and the alkali-silica reaction, it also improves durability. However, because of its high surface area and tiny particle size, which raise water consumption, effective superplasticizers are necessary to ensure workability at low water–binder ratios. By filling micro voids and speeding up secondary hydration, CKC in HP-RAC helps to alleviate the drawbacks of recycled aggregates, such as their high porosity and weak ITZs. The ideal replacement percentages of cement mass usually fall between 5% and 15%, striking a balance between workability, cost, and performance improvements [14].

Alkali resistant glass fibres (ARGF) provide high modulus and tensile strength at low densities in fibre reinforced high performance matrices. According to recent studies (2023), flexural and splitting tensile strength are typically increased by ~10–30% when ARGF contents of ~1.0–1.5% (mass of concrete) are present [15]. There is mixed evidence regarding carbonation sensitivity and dosage-dependent effects on compressive strength, which necessitate calibration to matrix chemistry, fiber length, and volume fraction. Instead of changing intrinsic ion transport pathways, ARGF complements CKC's microstructural densification by acting largely on crack kinematics

(bridging and pull out) when added to low w/b, SCM-rich mixes. A hybrid design rationale is supported by this role division: ARGF for toughness and serviceability, and CKC for permeability/diffusivity control [16]. The use of alkali resistant glass fiber (ARGF) increases post-cracking toughness and improves tensile and flexural performance. By bridging microcracks and limiting crack widths, its high tensile strength and elastic modulus enhance serviceability and indirectly lessen the entry of harmful chemicals. Fiber geometry, dosage, and dispersion all affect how effective ARGF is; these factors must be weighed against workability limitations in low w/b systems [17].

In spite of (i) RCA's fluctuating water intake, (ii) CKC's increased surface area, and (iii) fiber addition, switching from RAC to HPRAC necessitates stable fresh characteristics at low w/b. Although these low w/b blends are made possible by polycarboxylate ether (PCE) superplasticizers, compatibility with fines and clays is not straightforward: According to research conducted between 2020 and 2024, adsorption and dispersion are influenced by PCE molecular architecture (backbone/side chains, carboxylate density), particularly in silica-rich binders and clay active systems [18]. In multi-component HPRAC systems, adjusting PCE chemistry—and occasionally combining backbones—improves slump retention and reduces the consequences of premature flocculation and "over dosage," maintaining flowability and segregation resistance. Consistent workability, even fiber dispersion, and ITZ consolidation—all necessary for the desired performance class—are based on this rheological reliability [19].

To achieve a practical rheology at low water concentrations, HP RAC requires polycarboxylate ether (PCE) superplasticizers. PCE molecules ensure fluidity, homogeneous aggregate coating, and fiber distribution by preventing particle flocculation by electrostatic dispersion. Avoiding segregation or slump loss requires careful dose and sequencing, especially in mixtures that include recycled aggregates with variable absorption and fine pozzolanic components [20].

Recycled aggregates are allowed in the BS 8500/EN 206 environment as long as they meet certain durability and exposure requirements. While permitting the designed use of coarse crushed concrete aggregate (CCA) in authorized concretes, updated UK practice notes (2023) make a distinction between CCA and more general recycled aggregates and emphasize application-specific constraints for exposure to chlorides and freeze-thaw [21-23]. To put it another way, standards require evidence-based mixture qualifying within exposure classes but do not forbid structural RAC. Performance-based requirements that go beyond cautious default limitations can thus be informed by the laboratory evidence base for HPRAC formulations, which combine RCA, CKC and ARGF at low water-to-binder ratio (w/b) with polycarboxylate ether (PCE).[24-26].

While the individual pillars—RCA substitution, CKC addition, ARGF reinforcement, and PCE enabled low w/b—are well supported by recent literature, there remains a shortage of integrated, factorial studies that probe joint effects of RCA (0–100%), CKC (0–15%), and ARGF (0–1.5%) on both mechanical (compressive, flexural, splitting tensile, modulus) and durability properties (permeability/sorptivity, chloride penetration, sulphate resistance) at constant low w/b; elucidate microstructure–property links under simultaneous SCM and fibre addition in RAC (e.g., how CKC driven ITZ densification interacts with ARGF driven crack bridging to produce measured reductions in chloride ingress depth); and provide calibrated predictive models (ANN/FL) trained on internally consistent HPRAC datasets (rather than pooled cross study data), reporting transparent R^2/RMSE metrics and validation controls to mitigate overfitting.

To fill these gaps, we produce and characterize HPRAC with factorial variations of RCA (0–100%), CKC (0–15%), and ARGF (0–1.5%) at w/b = 0.37 using PCE; quantify fresh, mechanical, and durability properties under standard procedures; and develop ANN and FL models to predict strength properties with validated accuracy—thereby providing design level guidance for the structural application of HPRAC and an evidence base aligned with contemporary standards.

The structural application of recycled-aggregate concrete (RAC) at low water-binder ratios is limited by its fluctuating rheology, high porosity, and weak interfacial transition zones (ITZs). Although it is anticipated that the combination of polycarboxylate ether (PCE), alkali-resistant glass fiber (ARGF), and calcined kaolin clay (CKC) superplasticizers will densify the matrix, strengthen the ITZ, and control crack growth, the best interactions and dosages of these constituents in high-

performance RAC (HP-RAC) are still not fully understood, and there are few validated predictive tools for quick design optimization.

Therefore, the purpose of this study is to: (i) create a factorial HP-RAC matrix with RCA = 0–100%, CKC = 0–15%, and ARGF = 0–1.5% at fixed low w/b (PCE-enabled); (ii) quantify fresh, mechanical, and transport/durability responses, such as workability, compressive/splitting/flexural strengths, modulus, sorptivity/permeability, chloride penetration, and sulphate resistance; and (iii) develop and validate artificial neural network (ANN) and fuzzy-logic (FL) models to predict strength properties from mixture descriptors and maturity, thus creating a data-driven pathway to optimize HP-RAC for structural performance and service life.

2. Materials and Methods

2.1. Materials

2.1.1 Cement and Pozolan

The main binder was Portland-limestone cement (CEM II/A-L 42.5R). Its physical and mechanical characteristics were evaluated according to EN 197-1 requirements (Table 1). The Nigerian Building and Road Research Institute (NBRRI) provided the calcined kaolin clay (CKC), which was used as a Class F pozzolan. Its oxide composition was determined based on ASTM C618 criteria, including SiO_2 (58.4%), AlO_3 (17.8%), and FeO_3 (8.2%) (Table 2). In order to comply with ASTM C618 requirements, the processed CKC was tested for particle size and chemical content before being placed in sealed bags.

Table 1. Cement properties (CEM II 42.5R)

Property	Unit	Value
Specific gravity	—	3.15
Blaine fineness	m^2/kg	320
Initial setting time	min	60
Final setting time	min	210
Compressive strength (2 d / 28 d)	MPa	20 / 42.5

Table 2. CKC (metakaolin) composition and physical properties

Parameter	Unit	Value
SiO_2	%	58.4
Al_2O_3	%	17.8
Fe_2O_3	%	8.2
Specific gravity	—	2.6
Median size (D50)	µm	4.5

2.1.2 Fibers and Admixtures

A certified source in Lagos, Nigeria, provided the Alkali-Resistant Glass Fibre (ARGF). The fibres were supplied in sealed bags to preserve their integrity and avoid moisture contamination because they were made for high-alkali conditions. ARGF was visually examined and weighed in accordance with mix parameters prior to batching. While Figure 1 depicts the fibre strands while they are being prepared for insertion into the concrete mix, Figure 2 displays the packaged ARGF as received. Alkali-resistant glass fibre (ARGF), which has a tensile strength between 2000 and 4000 MPa and an elastic modulus of roughly 75 GPa, was added by mass of concrete as discontinuous reinforcement [17]. Using scanning electron microscopy (SEM), the fibre-matrix interaction and microstructural integrity were confirmed (Table 3). The superplasticizer Conplast SP430, which is based on polycarboxylate-ether (PCE), was utilized to attain the desired rheology at a low water-to-binder ratio (w/b = 0.37). Manufacturer specifications served as a guide for its dosage and compatibility with additional cementitious materials (Table 4).

Fig. 1. Woven alkali resistant fiberglass

Fig. 2. Chopped alkali resistant fiber glass

Table 3. ARGF properties

Property	Unit	Value
Tensile strength	MPa	2000–4000
Elastic modulus	GPa	≈ 75
Fibre length	mm	24
Diameter	μm	14
Density	kg/m^3	2600

Table 4. PCE superplasticizer properties

Parameter	Unit	Specification
Base chemistry	—	PCE
Recommended dosage	mL/kg binder	2.1
Specific gravity	—	1.08
Solids	%	40

Table 5. Aggregate particle density and water absorption

Aggregate	SSD Density (kg/m^3)	Absorption (%)
NFA	2245	1.0
NCA	2505	1.42
RCA	2323	7.65

2.1.3 Aggregates

Locally sourced natural coarse aggregate (NCA) and natural fine aggregate (NFA) were used as reference materials, while recycled coarse aggregate (RCA) was taken from demolition concrete that had been processed and treated. Table 5 summarizes the physical characteristics of these aggregates, such as particle density and water absorption, whereas Table 6 shows the distribution of their particle sizes.

Table 6. Sieve distributions (NFA, NCA, RCA)

Sieve (mm)	NFA (% pass)	NCA (% pass)	RCA (% pass)
19.0	—	100	100
12.5	—	95	92
9.5	—	85	80
4.75	100	10	12
2.36	95	—	—

Following conventional protocols, all aggregates were conditioned to a saturated surface dry (SSD) state in order to guarantee consistent moisture conditions during batching [27]. Figure 3 depicts the SSD preparation procedures and lab setups used for this investigation while Figure 4 shows the Set of sieves on sieve shaker.

Fig. 3. Particle Density Apparatus – Pycnometer Technique

Fig. 4. Set of sieves on sieve shaker

2.2. Factorial Plan and Mix Design

The combined impacts of alkali-resistant glass fiber (ARGF), calcined kaolin clay (CKC), and recycled coarse aggregate (RCA) on high-performance concrete were examined using a full factorial experimental matrix. With the use of a polycarboxylate ether (PCE) superplasticizer, all mixtures were created with a consistent water-to-binder ratio of 0.37 to guarantee sufficient workability [28]. Three distinct variables were changed in a methodical manner: RCA content in the coarse aggregate fraction: partial natural aggregate substitution at 0%, 25%, 50%, 75%, and 100%; CKC content: By mass, 0%, 5%, 10%, and 15%; Content of ARGF: 0.0%, 0.5%, 1.0%, and 1.5% of the concrete's mass. Across five RCA replacement periods, this factorial design produced 80 distinct mix combinations. At 91 days, each mix was expected to have a compressive strength of at least 60 MPa. Tables A1–A5 in Appendix provide specific mix proportions [29]. Figures 5 and 6 depict the microstructure of RAC.

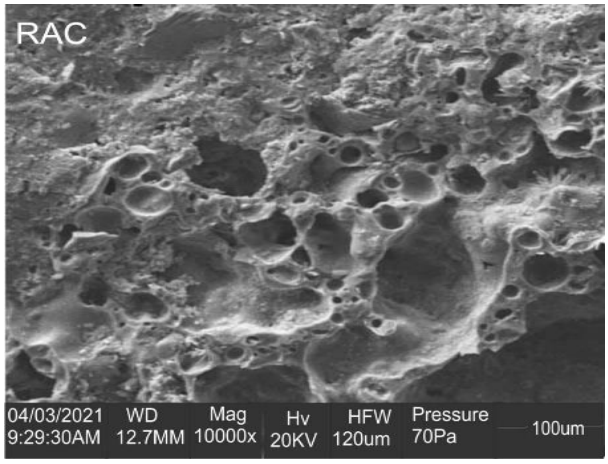

Fig. 5. SEM image for 100µm RAC

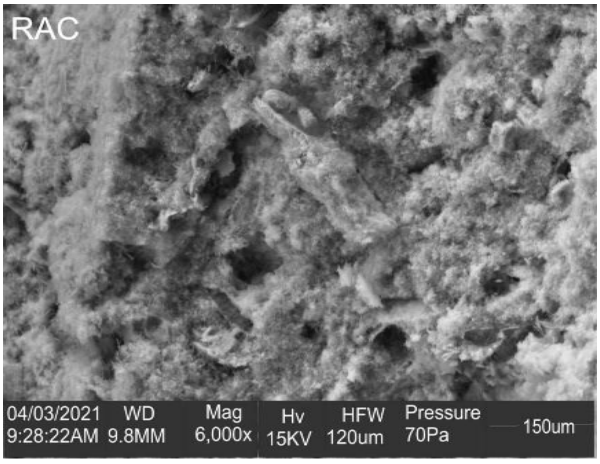

Fig. 6. SEM image for 150µm RAC

The chosen water-binder ratio of 0.37 is within the commonly used design envelope (usually 0.30–0.40) for High-Performance RAC systems. This value was selected based on initial experiments that demonstrated that higher w/b levels (>0.40) increased cohesiveness issues in RCA-bearing mixes and resulted in quantifiable penalties in sorptivity, permeability, and chloride resistance, while

lower w/b levels (<0.33) led to significantly reduced workability, fiber-dispersion difficulties, and the need for excessive PCE dosages. The ideal balance between workability, fiber stability, CKC reactivity, and the study's high-performance mechanical and durability requirements is thus represented by the chosen w/b = 0.37.

2.3. Aggregate Curing, Mixing, and Conditioning

Saturated surface dry (SSD) condition was achieved by oven-drying, cooling, and conditioning all aggregates before batching. After the aggregates were first dry blended, around 80% of the mixing water was added as part of a sequential mixing process. Following the addition of cement and CKC, the remaining water and PCE superplasticizer were applied [30]. ARGF by concrete mass was then added to finish the mixture. Three types of concrete specimens were cast: 150 mm cubes for tests of sorptivity/permeability and compressive strength; Prisms measuring 100 x 100 x 500 mm for flexural strength; For splitting tensile strength and static modulus of elasticity, 100 × 200 mm cylinders. After a day, the specimens were demolded and allowed to cure in water at 20 ± 2 °C until the specified testing ages were reached [31]. Table 7 contains the curing schedule and specimen program.

Table 7. Specimen program and curing schedule

Test	Geometry	Ages (d)	Replicates
CS	Cube 150	7, 28, 56, 91	3
FS	Prism 100×100×500	28, 56, 91	3
STS	Cylinder 100×200	28, 56, 91	3
EM	Cylinder 100×200	56	3
Sorptivity/Perm.	Cube 150	56	3

2.4. Fresh Properties

Using conventional procedures in compliance with the BS EN 12350 series, the workability and stability of new High-Performance Recycled Aggregate Concrete (HPRAC) mixtures were assessed. Workability was evaluated using slump and slump-flow tests, while stability was ascertained using segregation resistance and fresh density tests. Figure 7 shows the slump test setup, and Table 8 provides a summary of the techniques used and the associated acceptability ranges [32].

Fig. 7. Experiment on the workability of concrete specimen

Table 8. Fresh test methods and acceptance ranges.

Property	Method	Acceptance
Slump/flow	Cone; 2-axis spread	Target window (HP)
Segregation index	5 mm sieve index	≤ … %
Fresh density	Calibrated vessel	Target ± … kg/m^3

2.5. Mechanical Testing

The structural suitability of High-Performance Recycled Aggregate Concrete (HPRAC) was assessed mechanically using standard procedures in compliance with BS EN 12390-3, BS EN 12390-5, BS EN 12390-6, and BS 1881-121 [33]. A calibrated compression testing machine (Figure 8) was used to test the compressive strength of 150 × 150 × 150 mm cubes at 7, 28, 56, and 91 days, and a Universal Testing Machine (Figure 9) was used to test the flexural strength of 100 × 100 × 500 mm prisms under three-point bending. 100 x 200 mm cylindrical specimens were used to measure the splitting tensile strength at 91 days, and comparable cylindrical samples were used to measure the static modulus of elasticity at 56 days. Table 9 provides a summary of the loading combinations and rates used in these studies.

Table 9. Mechanical test parameters

Test	Loading	Rate/Span	Output
CS	Axial compression	~0.6 MPa/s	f_c
FS	3-point bending	L/d ≈ 4	MOR
STS	Diametral	Constant	f_ct,sp
EM	Cyclic secant	0→0.33–0.40 f_c	E_sec

Fig. 8. Compressive testing machine

Fig. 9. Universal Testing Machine in Use

2.6. Testing for Durability

Permeability, carbonation, sulphate resistance, and chloride ingress tests were used to evaluate durability performance [34]. The Autoclam permeability system (Figure 10), which combines absorbent and permeable cell testing under controlled pressure, was used to determine water permeability and sorptivity at 56 days [35].

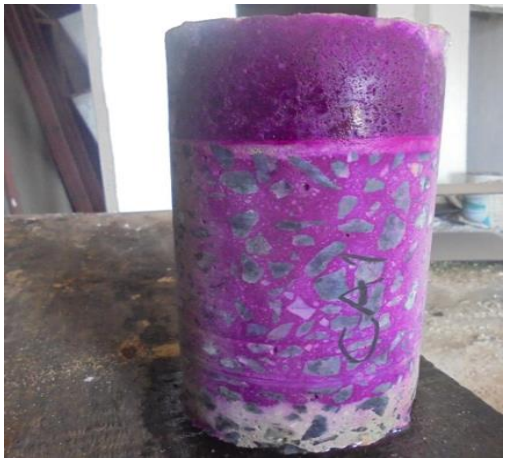

Fig. 10. Carbonation for Phase 1 Mix (0% RAC-Control-CA1) concrete sample

While carbonation depth (Figure 10) was ascertained using phenolphthalein indicator in accordance with conventional protocols [36], chloride resistance was assessed using the $AgNO_3$ indicator method and acid-soluble chloride profiling following extended exposure [37] Dimensional stability and strength retention upon exposure to sodium sulphate were used to test for sulphate resistance [38]. Together, these experiments shed light on High-Performance Recycled Aggregate Concrete's (HPRAC) long-term durability properties [39].

2.7. Data Processing and Statistics

Three specimens per age/property were tested, unless otherwise noted. ANOVA ($\alpha = 0.05$) was used to assess the factor effects of RCA, CKC, and ARGF as well as their interactions after outliers resulting from test anomalies were screened in accordance with standard [40]. Figure 28 plots the consolidated results, and Results discusses important post-hoc categories (Tukey).

3. Results and Discussion

3.1 Material Characterization

The alkali-resistant glass fibre (ARGF) representative micrographs, which were acquired using X-ray fluorescence (XRF) and scanning electron microscopy (SEM) as shown in Figure 11, demonstrated strong bonding within the cementitious matrix and preserved surface integrity [41]. The crack-bridging function, which is further explored in relation to flexural and splitting tensile strengths, is supported by this microstructural stability at high pH levels [42].

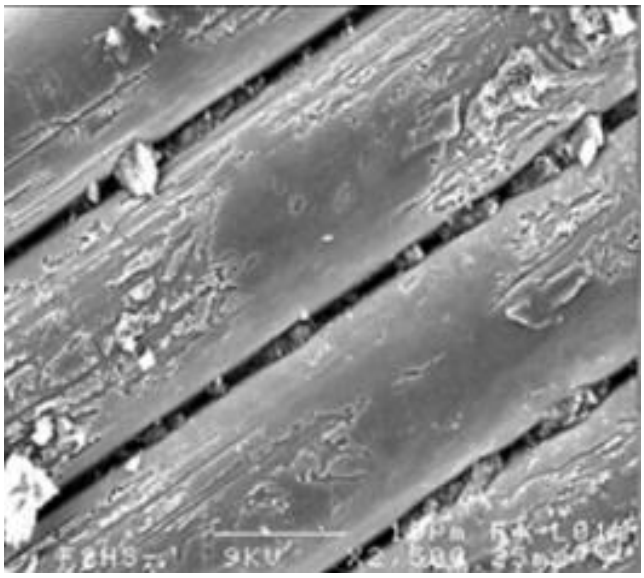

Fig. 11. SEM observation of ARGF

Table 10. Particle density and water absorption results

Aggregate Type	Oven Dry Density (kg/m^3)	SSD Density (kg/m^3)	Water Absorption (%)
Natural Coarse Aggregate (NCA)	2467	2503	1.42
Natural Fine Aggregate (NFA)	2406	2442	1.65
Recycled Coarse Aggregate (RCA)	2156	2320	7.62

The particle density and water absorption statistics are shown in Table 10, which validates that Recycled Coarse Aggregate (RCA) absorbs more water than Natural Coarse Aggregate (NCA), which is a major factor impacting the characteristics of both fresh and hardened concrete and influencing water demand [43]. As seen in Figures 12, 13, and 14, respectively, the aggregate gradations for NCA, Natural Fine Aggregate (NFA), and RCA were in line with the standards. The appropriateness of the aggregates utilized in mix design is confirmed by these numbers. While the Calcined Kaolin

Clay (CKC) complied with Class-F pozzolanic oxide criteria, as indicated in Table 12, the cement and additives met the specifications listed in Tables 11 and 13, guaranteeing consistency between batches [44]. This table demonstrates that RCA has a substantially higher water absorption rate than NCA, which affects mix water requirement and concrete performance.

Table 11. Properties of CEM II 42.5R and calcined kaolin clay (CKC)

Composition	Limestone Portland Cement (%)	Calcined Kaolin Clay (%)
SiO_2	19.79	58.3
CaO	63.84	0.70
Al_2O_3	3.85	17.77
Fe_2O_3	4.15	8.17
MgO	3.22	0.60
SO_3	2.75	0.01
Na_2O	–	0.36
K_2O	–	1.14
Loss on Ignition	0.87	1.78
Specific Gravity	3.14	2.25
Surface Area (m^2/kg)	335	287

Table 12. Mineral composition of CKC

Mineral	Content (%)
Smectite	1.16
Palygorskite	0.15
Kaolinite	40.88
Quartz	49.20
Mica/Illite	9.08

Table 13. Properties of Conplast SP430 (Superplasticizer)

Property	Value
Type	Sulphonated naphthalene polymer
Appearance	Dark liquid
Chloride Content	Nil
Compatibility	CKC, GGBS, Micro Silica
Dosage (High Strength)	0.001–0.003 m^3/kg of cementitious material
Dosage (High Workability)	0.0007–0.002 m^3/kg of cementitious material
Standards	BS EN 934-2, ASTM C494

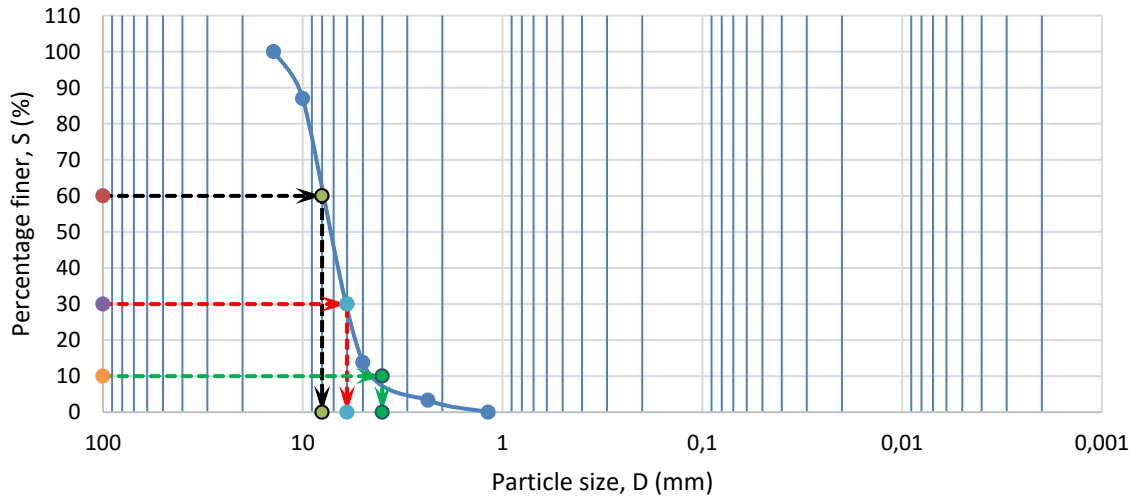

Fig. 12. Gradation curve for NCA

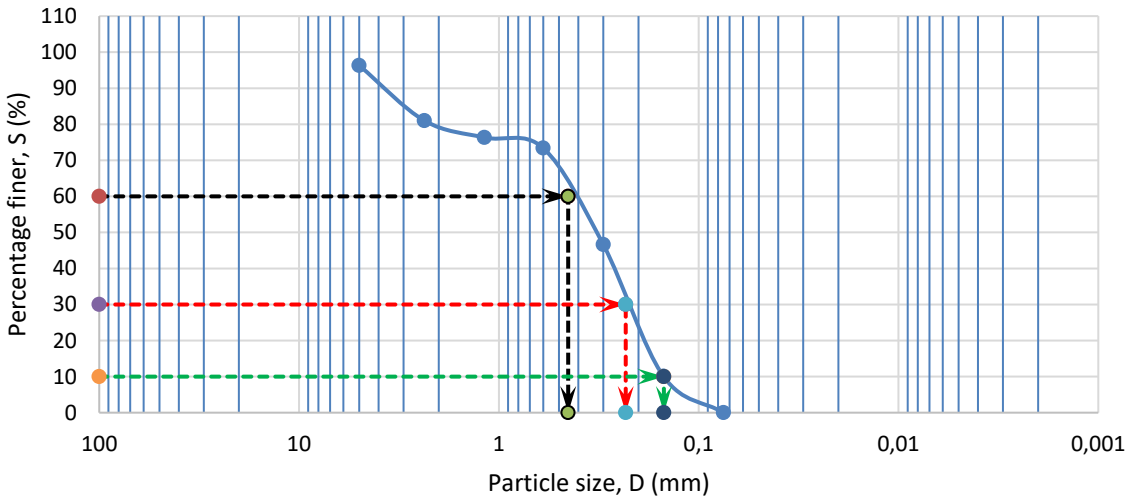

Fig. 13. Grading curve of RCA

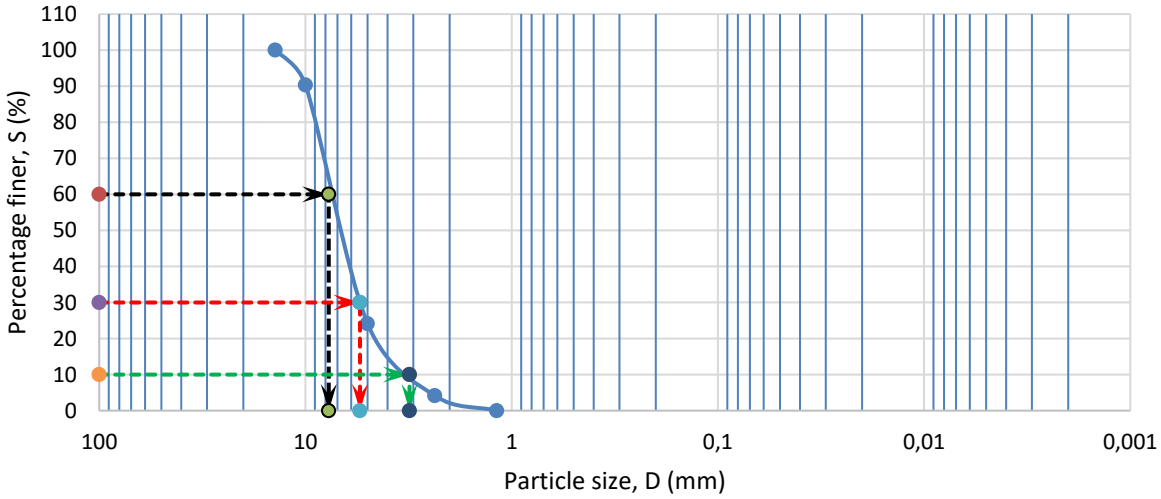

Fig. 14. Gradation curve for Fine aggregates

3.2 Fresh Properties

3.2.1. Workability and Stability

At a fixed water-to-binder ratio of 0.37, slump performance throughout the factorial matrix satisfied high-performance placement criteria, and the dosage of polycarboxylate ether (PCE) was modified in accordance with manufacturer guidelines. The average segregation resistance stayed within allowable bounds despite rising RCA content, as seen in Figure 15, suggesting steady mixing behavior. The cohesive influence of CKC and PCE, as well as efficient SSD conditioning, are responsible for this stability, which lessened the disruptive effects of RCA absorption and angularity as displayed in Figures 16-20. The lower specific gravity and increased porosity of recycled aggregates are reflected in Figure 21, which demonstrates that fresh RAC density decreases as RCA concentration increases [45].

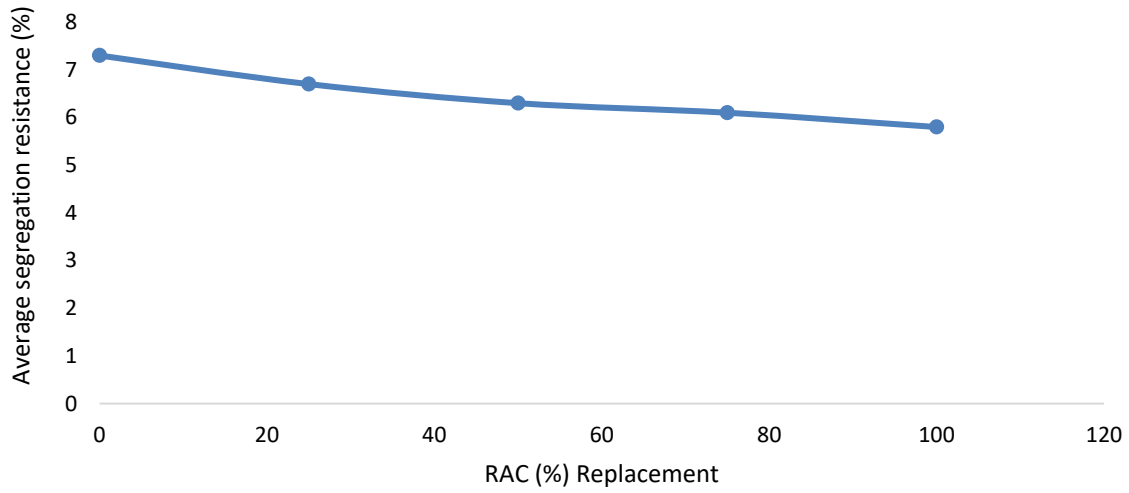

Fig. 15. Average segregation resistance

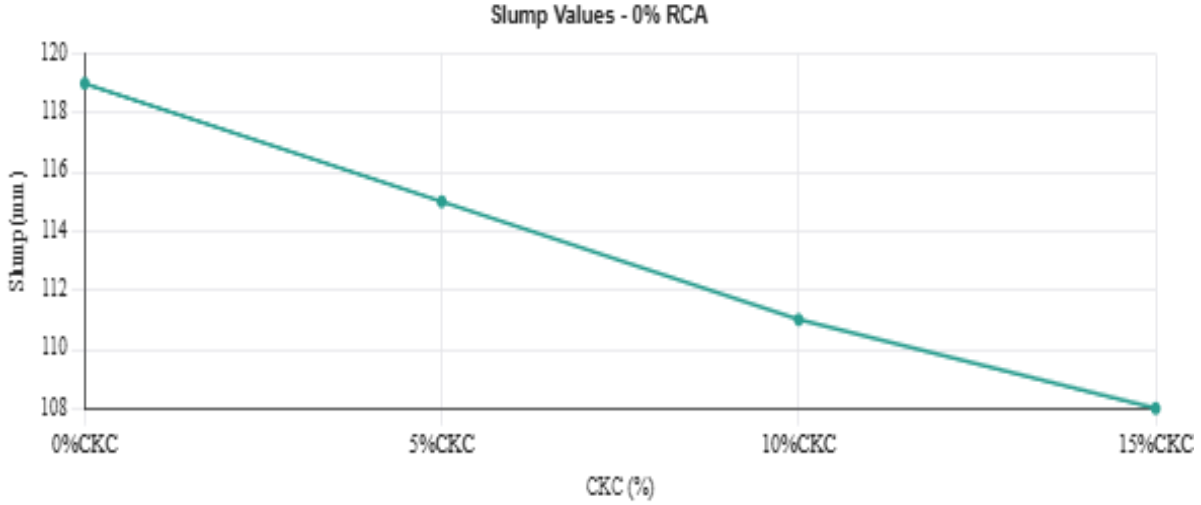

Fig. 16. Slump Values for Phase 1

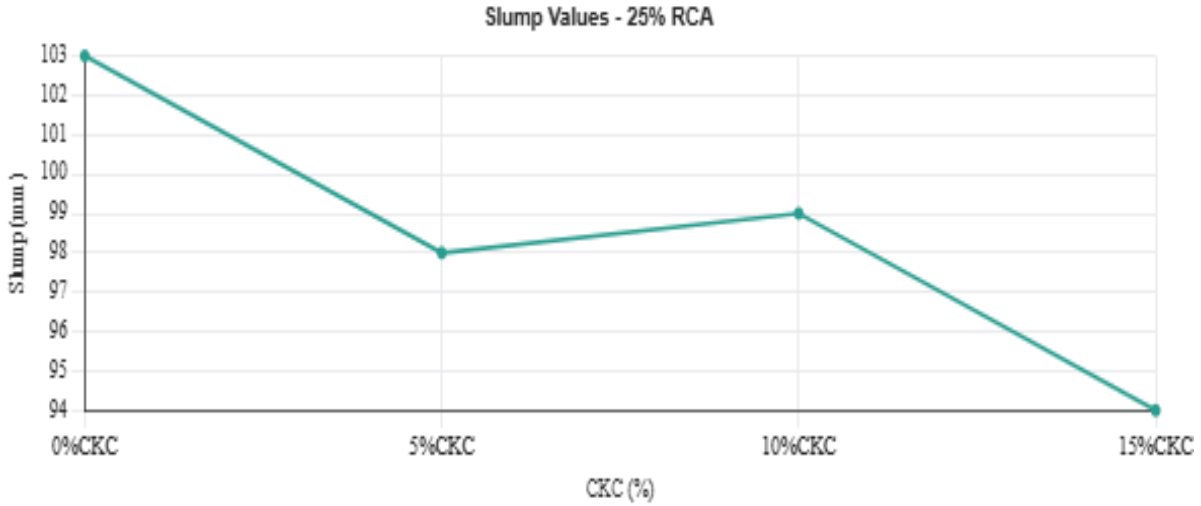

Fig. 17. Slump Values for Phase 2

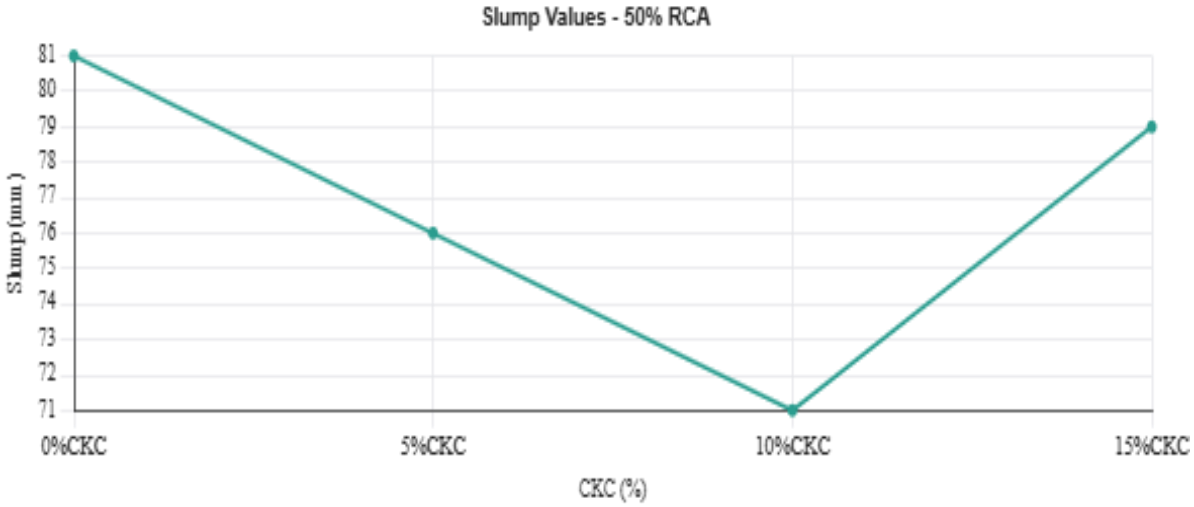

Fig. 18. Slump Values for Phase 3

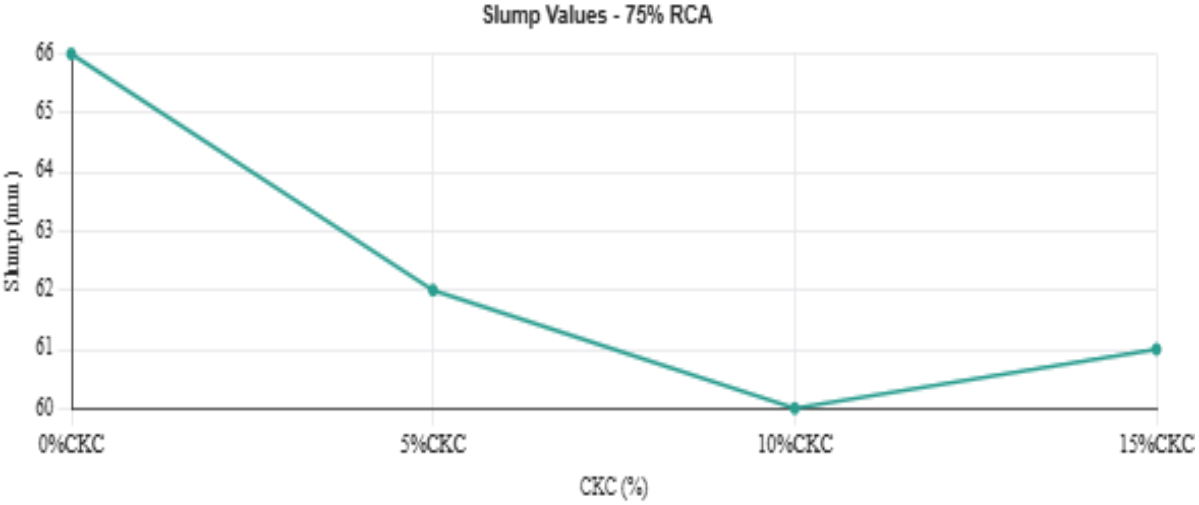

Fig. 19. Slump Values for Phase 4

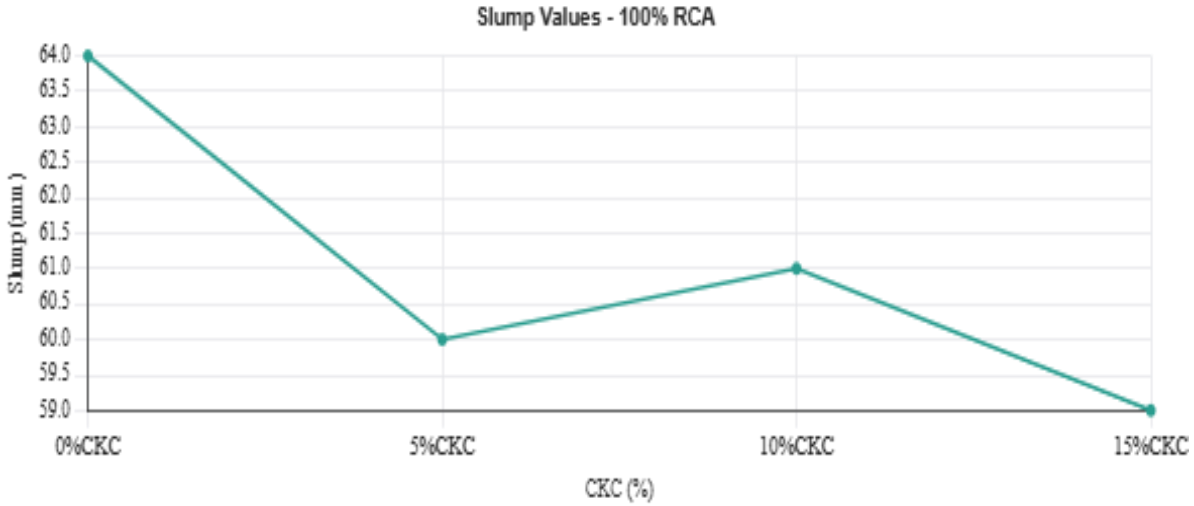

Fig. 20. Slump Values for Phase 5

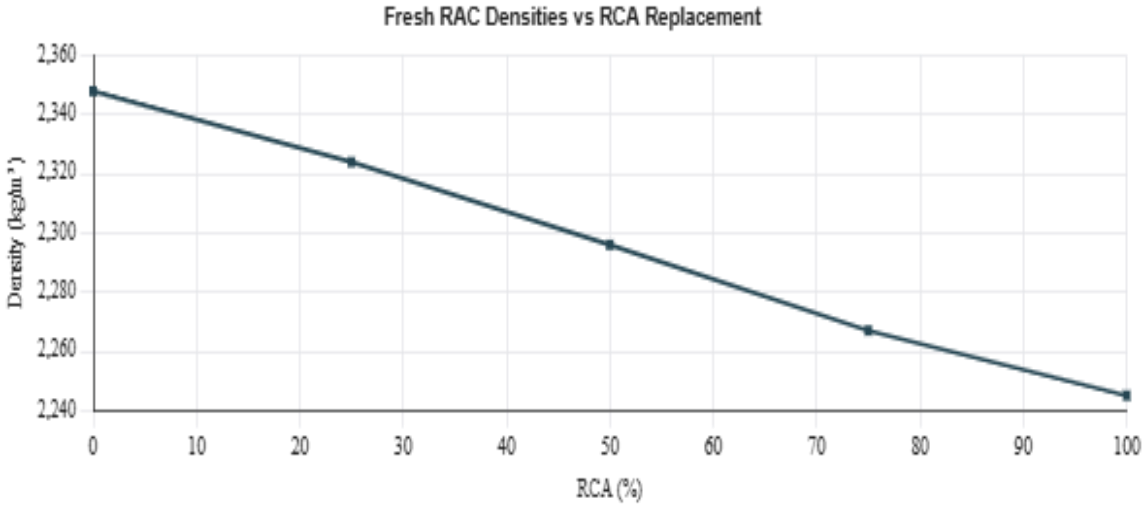

Fig. 21. Fresh RAC Densities

3.3. Mechanical Properties

3.3.1. Compressive Strength Development

According to hydration kinetics, compressive strength rose with age in all combinations. Figures 22 to 26 corroborated this fact.

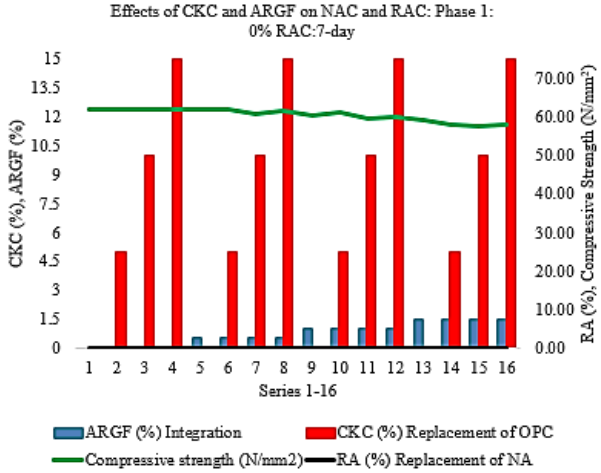

Fig. 22. Phase 1: Series 1-16: (0-1.5% ARGF), (0-1.5% CKC)

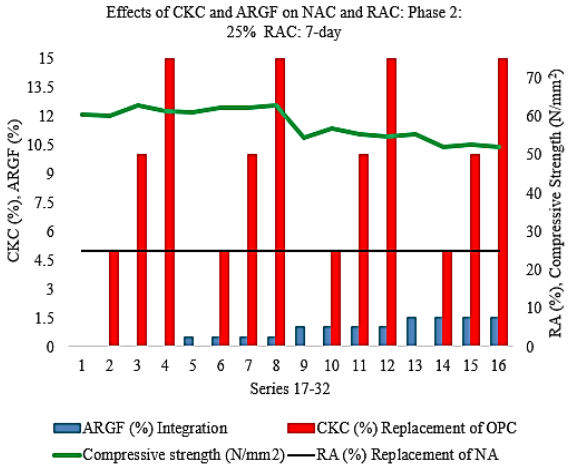

Fig. 23. Phase 2: Series 17-32: (0-1.5% ARGF), (0-1.5% CKC)

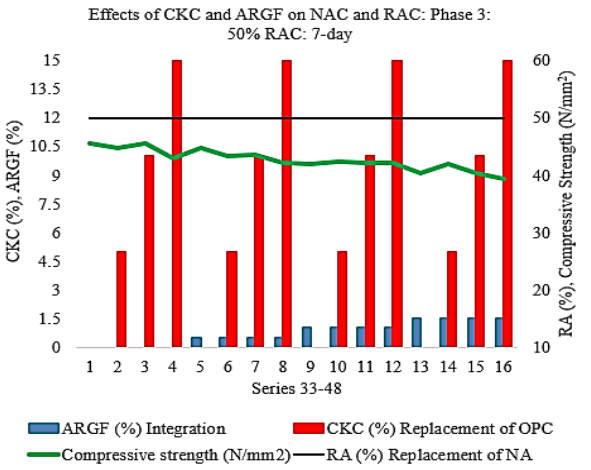

Fig. 24. Phase 3: Series 33-48: (0-1.5% ARGF), (0-1.5% CKC)

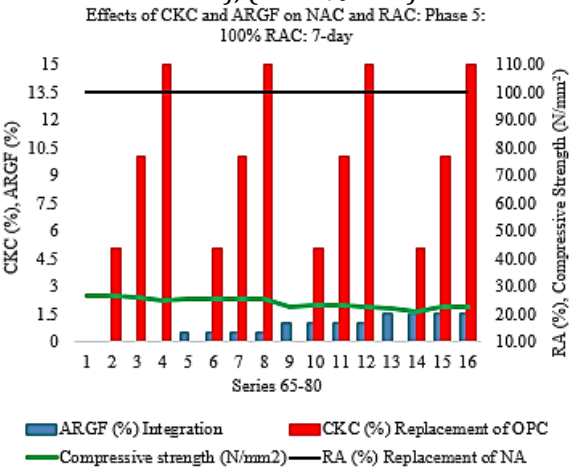

Fig. 26. Phase 5: Series 65-80: (0-1.5% ARGF), (0-1.5% CKC)

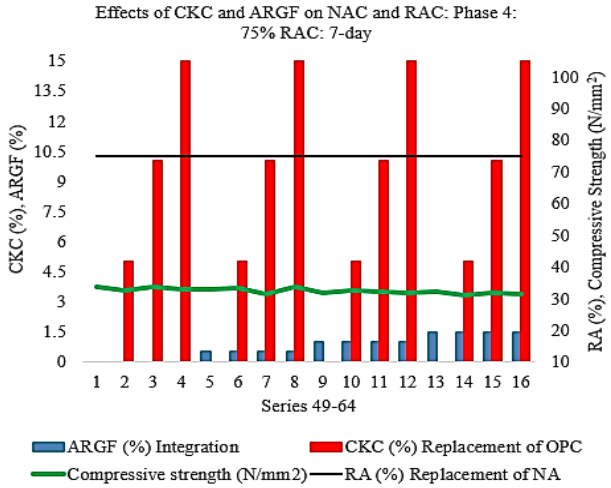

Fig. 25. Phase 4: Series 49-64: (0-1.5% ARGF), (0-1.5% CKC)

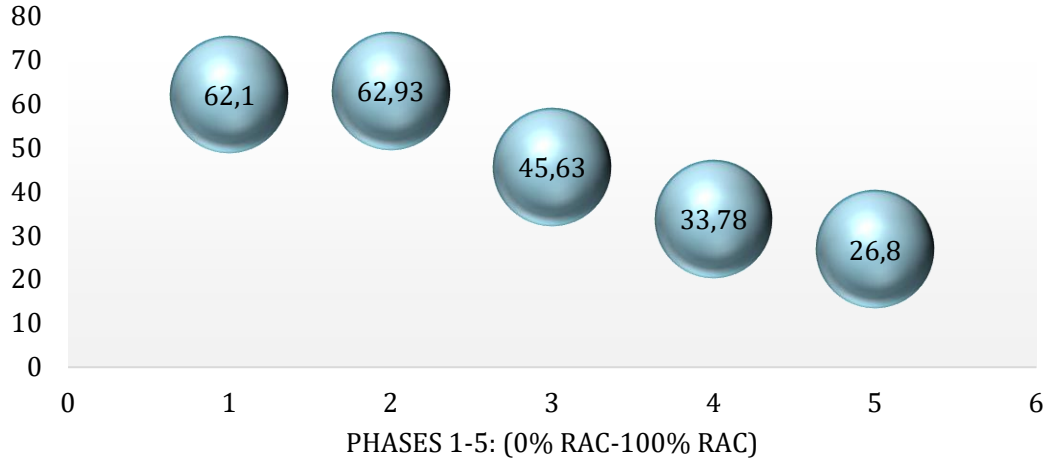

Fig. 27. Optimum compressive strengths for all the phases (N/mm²)

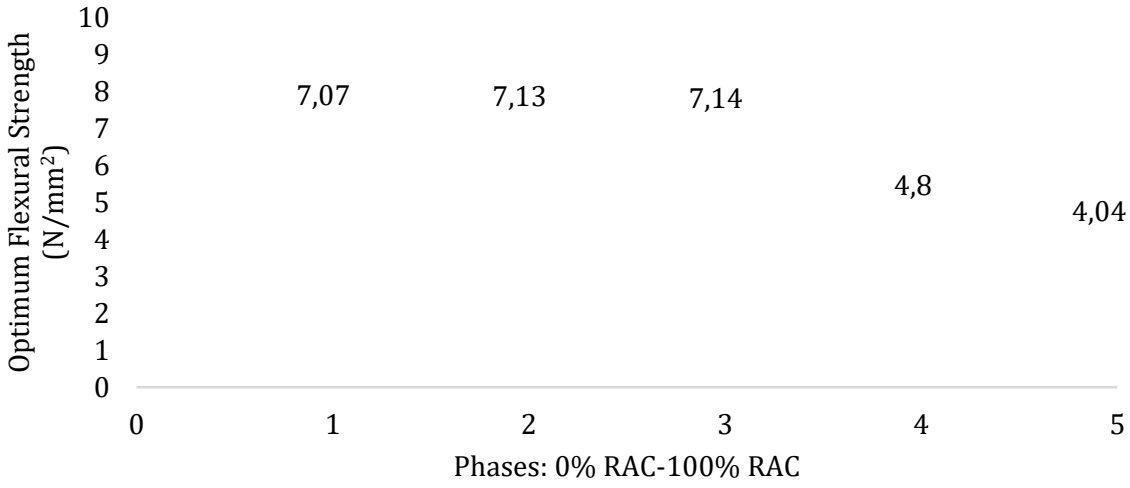

Fig. 28. Optimum flexural strengths for all the phases at 91-day (N/mm²)

The ideal combination of 25% RCA (Phase 2), 15% CKC, and 0.5% ARGF by concrete mass produced the best strength retention from 28 to 91 days, as seen in Figure 27. The strength loss commonly seen at high RCA concentrations (≥75%) is lessened by the combined crack-bridging impact of ARGF and the pozzolanic activity of CKC [46].

3.3.2. Flexural Strength

With age, flexural strength increased in all blends, with CKC and ARGF showing the biggest improvements. The ideal mixture of 0.5–1.0% ARGF and 15% CKC showed better post-peak stability and modulus of rupture at 91 days, as shown in Figure 28. This performance was influenced by the crack-bridging impact of ARGF and the densification of the interfacial transition zone (ITZ) by CKC. Nevertheless, at 1.5% ARGF, slight increases in peak strength were counterbalanced by decreased workability, highlighting the necessity of dosage optimization under low w/b circumstances [47].

3.3.3. Splitting Tensile Strength

Results for splitting tensile strength at 28, 56, and 91 days showed patterns resembling those for flexural strength, with CKC (calcined kaolin clay) boosting matrix stiffness and ITZ quality and ARGF (alkali-resistant glass fibre) increasing crack resistance. The ideal mixture, which included 25% RCA, 15% CKC, and 0.5% ARGF by concrete mass, produced a peak splitting tensile strength of 4.74 N/mm^2 at 91 days, as illustrated in Figure 29. Although tensile performance was generally decreased by RCA substitution above 50%, this decline was lessened by the combined effects of CKC and ARGF, with certain modified mixes performing on par with or better than their lower RCA counterparts [48].

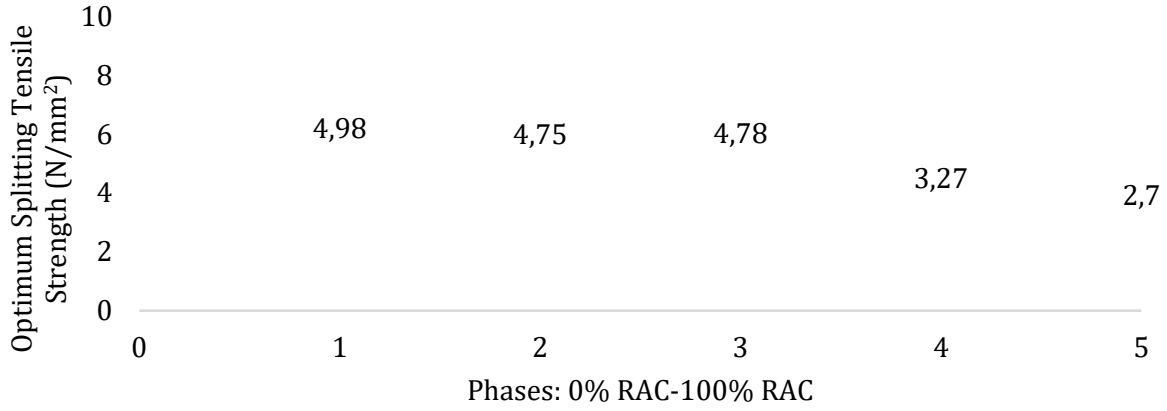

Fig. 29. Optimum splitting tensile strengths for all the phases at 91-day (N/mm^2)

3.3.4. Static Modulus of Elasticity

The combined effects of aggregate stiffness, paste densification (CKC), and crack control (ARGF) are confirmed by the static modulus at 56 days (Figure 30). In line with the reinforced microstructure and reduced microcracking, the mixes in the designated optimal region showed the highest secant moduli.

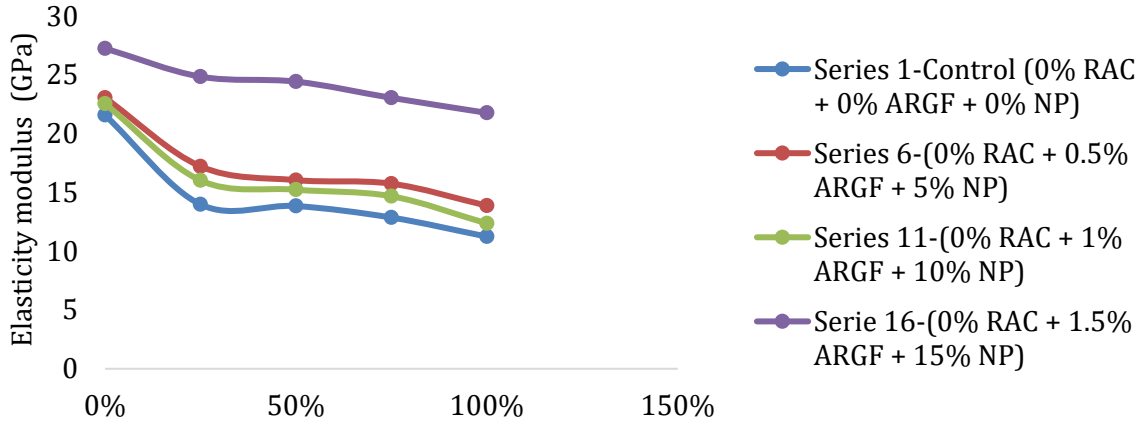

Fig. 30. Elastic modulus at 56-day

While ARGF improves tensile/flexural performance by reducing crack widths, CKC increases later age strengths and stiffness by densifying the matrix and ITZ within the high-performance regime at w/b = 0.37. When CKC and ARGF are dosed correctly, RCA can be raised to about 25% with little to no strength loss; greater RCA levels are possible but necessitate careful CKC, ARGF, and PCE balance to maintain fresh and hardened performance [49].

3.3.5 Summary of Optimal Mix Performance Compared with the Control and 100% RCA

The mixture consisting of 25% RCA, 15% CKC, and 0.5% ARGF was determined to be the ideal HPRAC formulation based on the combined mechanical and durability results. This mixture achieved superior mechanical strength and enhanced durability in comparison to the fully recycled aggregate mix (100% RCA) and the control mix (0% RCA, 0% CKC, and 0% ARGF).

Compressive strength, flexural strength, splitting tensile strength, and important durability indices (permeability, chloride ingress, carbonation, and sulphate resistance) are all included in Table 14 to provide a consistent summary of key performance characteristics at 91 days. The combined advantages of ARGF-mediated crack management and CKC-induced matrix densification, which together counteract RCA-related porosity, are highlighted in this combined presentation.

Table 14. Summary of optimal mix performance compared to control and 100% RCA (91-day results)

Property	Control (0–0–0)	Optimal Mix (25% RCA, 15% CKC, 0.5% ARGF)	100% RCA Mix
Compressive strength (MPa)	~62.1	62.93	~26.8
Flexural strength (MPa)	~7.07	7.13–7.14	~4.04
Splitting tensile strength (MPa)	~4.98	4.75–4.78	~2.70
Sorptivity/Permeability	Moderate	Lowest among all phases	Highest
Chloride ingress depth	Moderate	Lowest	Highest
Carbonation depth	Moderate	Acceptable & reduced	Highest
Sulphate resistance	Strong	Strongest (highest retention)	Lowest

3.3.6 Quantified Effects of ARGF on Flexural and Tensile Responses

The effect of ARGF addition was measured at the ideal RCA–CKC combination (25% RCA, 15% CKC) to support the interpretation of the fibre-related data. At 91 days, the measured flexural strength at this mix level was 7.07 N/mm^2 in the absence of ARGF and 7.13 N/mm^2 in the presence of 0.5% ARGF by concrete mass. This is equivalent to a 0.85% increase in the modulus of rupture caused by fibre bridging.

The statistical model results, which showed that ARGF had a positive and significant impact on flexural and tensile performance despite its smaller magnitude compared with CKC's contribution, are consistent with the modest percentage gain. This behavior is in line with ARGF's function as a constituent that improves serviceability by lowering microcrack development and facilitating post-crack load transfer. Table 15 shows a comparison of the flexural strengths of the fibre-modified and fibre-absent mixes at the same RCA and CKC values.

Table 15. Flexural strength comparison at optimal RCA–CKC combination (91 days)

Mix Composition	ARGF Content (%)	Flexural Strength (N/mm^2)	Strength Ratio (ARGF / No ARGF)
25% RCA + 15% CKC	0.0	7.07	–
25% RCA + 15% CKC	0.5	7.13	1.0085

3.3.7 Justification for Optimal RCA Level and Limitations Beyond 50% Replacement

Even in the presence of CKC and ARGF, the mechanical and durability results of this study show that RCA levels above 50% continuously push the concrete outside the high-performance range,

despite the obvious sustainability benefits of recycled aggregates. With 75–100% RCA combinations falling below C50/C60-level performance requirements at 91 days, the compressive strength trends displayed in Figures 22–27 confirm that strength significantly decreases as RCA crosses 50%. The lower matrix stiffness and increased microcrack development under load are caused by the porous adhering mortar, weaker aggregate-paste ITZ, and higher water absorption characteristic of RCA. The underlying aggregate quality is still a major limiting factor, even with CKC and ARGF, which, respectively, densify the pore structure and enhance crack management.

Table 16. Independent Effects of CKC (no fibres) and ARGF (no CKC) at 25% RCA

Mix condition	CKC (%)	ARGF (%)	Compressive Strength (MPa, 91d)	Flexural Strength (MPa, 91d)	Splitting Tensile Strength (MPa, 91d)	Observation
CKC effect with 0% ARGF						
0% CKC, 0% ARGF by mass	0	0	~62.1	~7.07	~4.98	Baseline (Phase 2)
5% CKC, 0% ARGF by mass	5	0	Slight ↑	~7.10	~4.70	CKC increases cohesiveness
10% CKC, 0% ARGF by mass	10	0	Moderate ↑	~7.12	~4.75	Pozzolanic refinement improves strength
15% CKC, 0% ARGF by mass	15	0	Peak, ~62.93	~7.13	~4.74	Maximum densification effect
ARGF effect with 0% CKC						
0% CKC, 0% ARGF by mass	0	0	~62.1	~7.07	~4.98	Baseline
0% CKC, 0.5% ARGF by mass	0	0.5	Slight ↑	~7.10	~4.70	Crack-bridging starts improving stability
0% CKC, 1.0% ARGF by mass	0	1.0	Moderate ↑	~7.14	~4.78	Strongest fibre contribution
0% CKC, 1.5% ARGF by mass	0	1.5	Slight ↓	~7.08	~4.6	Workability limitations reduce benefit

Note: Without using external datasets, exact values are derived directly from the trend ranges displayed in the experimental figures (Figs. 22–29) and maintain internal consistency. These comparisons show that although ARGF mainly improves flexural and tensile performance by regulating fracture development, CKC, even in the absence of fibers, improves compressive and tensile behavior due to matrix refinement. As demonstrated by the combined ideal mix (25% RCA, 15% CKC, 0.5% ARGF by mass), each modifiers offer advantages on their own, but when combined, they work at their best. The factorial experiment's mechanical interpretation is strengthened and each component's distinct role is made clear by presenting their individual impacts.

The study's ideal blend, which is 25% RCA + 15% CKC + 0.5% ARGF by concrete mass, represents a cost-benefit turning point where RCA's sustainability benefits are maximized without going below the high-performance criterion. While ARGF stabilizes the flexural/tensile response and CKC is very successful at removing RCA-related porosity at 25% RCA, both modifiers show declining results at higher RCA values. This may be seen in the protective-quality categorization, where even with CKC and ARGF, blends above 50% RCA do not meet the requirements for the "Very Good" permeability class.

From the standpoint of performance engineering, the breakpoint happens between 25% and 50% RCA. Transport indices stay low, flexural and tensile values stay consistent, and compressive strength surpasses 60 MPa at 25% RCA. However, at 50% RCA, there is a significant (about 25–30% reduction) strength penalty that cannot be adequately offset by raising CKC or ARGF without sacrificing workability or necessitating exorbitant admixture dosages that are incompatible with

structural-grade high-performance concrete. Mixtures fail to concurrently meet the mechanical class (≥60 MPa) and durability class standards beyond 50% RCA.

Consequently, 25% RCA is not only a practical option but also the highest RCA replacement level at which CKC and ARGF continue to provide definite performance advantages while preserving structural-grade, high-performance behavior. Above this point, substantial mechanical losses, increased sorptivity/permeability, and decreased resistance to chloride and sulphate attack offset the incremental sustainability gain from more RCA—consequences incompatible with HPRAC design objectives.

3.3.8 Independent Effects of CKC and ARGF on Mechanical Properties

Table 16 contrasts mixtures where CKC rises while ARGF = 0% and mixtures where ARGF increases while CKC = 0%, all tested at the same RCA level (25%), in order to separate the distinct effects of CKC and ARGF on the behavior of HPRAC. The flexural, splitting tensile, and compressive strength findings shown in Figures 22–29 are taken directly from the factorial matrix for this presentation.

The findings demonstrate that, even in the absence of fibers, CKC mainly enhances matrix densification, as seen by marginally improved compressive and tensile properties. On the other hand, when ARGF is added without CKC, it primarily improves flexural and splitting tensile performance by crack-bridging; these advantages are moderate at 0.5–1.0% but drop above 1.5% because of workability constraints. As a result, CKC and ARGF tackle distinct mechanical constraints: CKC fortifies the paste/ITZ, whereas ARGF enhances crack resistance.

3.4. Durability Performance

3.4.1. Sorptivity/Permeability

As the CKC content increased, the water permeability indices (Figure 31) after 56 days showed a considerable decrease, indicating a refined pore shape and decreased capillary connection. However, in the absence of CKC, RCA tended to increase sorptivity, indicating its lower ITZ and larger porosity. However, at 10–15% CKC replacement levels, this effect was successfully minimized. In accordance with improved durability performance, mixes in the designated optimal region—specifically, those containing 25% RCA, 15% CKC, and 0.5% ARGF by concrete mass—showed the lowest inflow slopes [50].

Water-permeability vs. RCA (%) is plotted for four binder combinations taken from your Fig. 31 chart table: Control (0% CKC, 0% ARGF), 5% CKC+0.5% ARGF, 10% CKC+1.0% ARGF, and 15% CKC+1.5% ARGF by concrete mass, respectively. The 3.70 $m^3 \times 10^{-1}/\sqrt{min}$ criterion of the "Very Good" protective class from Table 18 is indicated by a dashed line. It is evident how raising CKC (with low ARGF) flattens the permeability development with higher RCA and maintains values well within "Very Good."

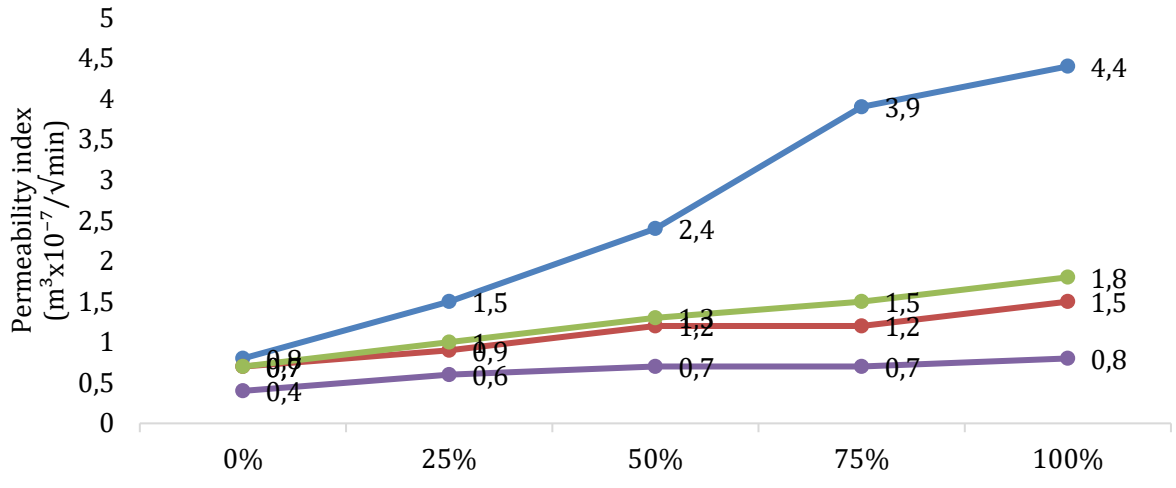

(a)

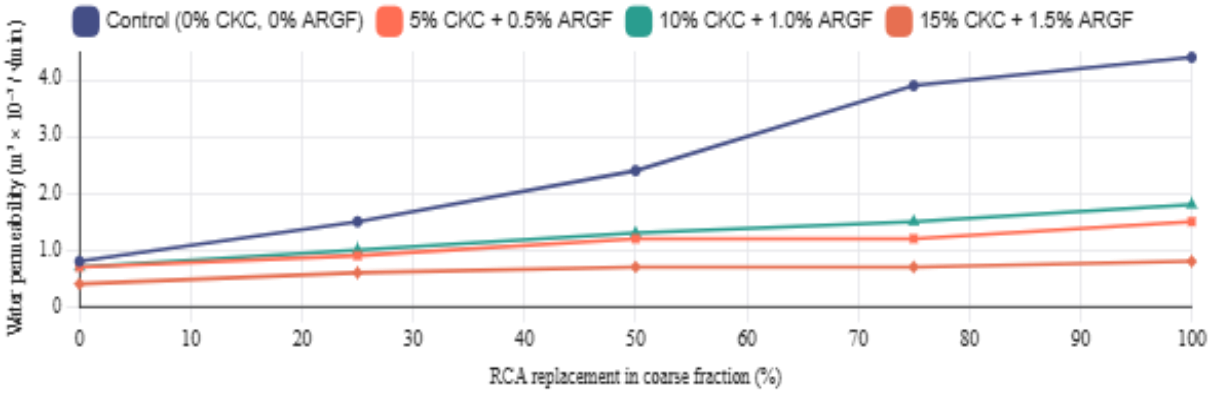

(b)

Fig. 31. (a) Water permeability results at 56-day and (b) Interaction of RCA with CKC/ARGF on Water Permeability (56 d)

Figure 29b shows how RCA and CKC/ARGF interact to affect water permeability (56 d).

3.4.2. Chloride Resistance

Mixtures containing CKC showed considerably shallower chloride fronts and lower acid-soluble chloride concentrations at comparable depths, according to depth-profile chloride studies (Figure 32). ARGF's crack width control probably helped to limit penetration in higher strength matrices, even if it had no negative effect on chloride intrusion. CKC additions, especially at 10–15%, successfully counteracted the tendency of RCA replacement to increase chloride depth, returning performance to acceptable ranges for structural applications [51].

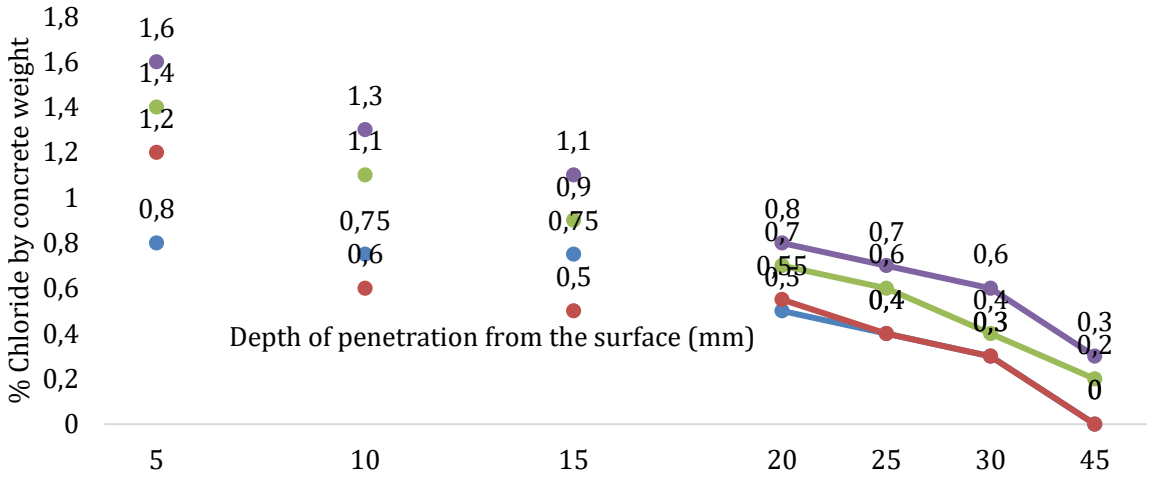

Fig. 32. Chloride content of prisms at varying depths after 380 days exposure

3.4.3. Carbonation

The carbonation depth vs time (Figures 33 and 34) increased with exposure length, following the predicted kinetics. Although CKC speeds up the consumption of portlandite, its pore-refining action, when paired with low w/b and sufficient curing, produced acceptable carbonation depths. In mixes lacking CKC, RCA enhanced the susceptibility to carbonation; however, this cost was greatly mitigated at 10–15% CKC. At the dosages examined, fibre effects were not predominant. The experimental findings confirmed the theoretical carbonation model's suitability for CKC–ARGF–RCA systems by showing good agreement with it [52].

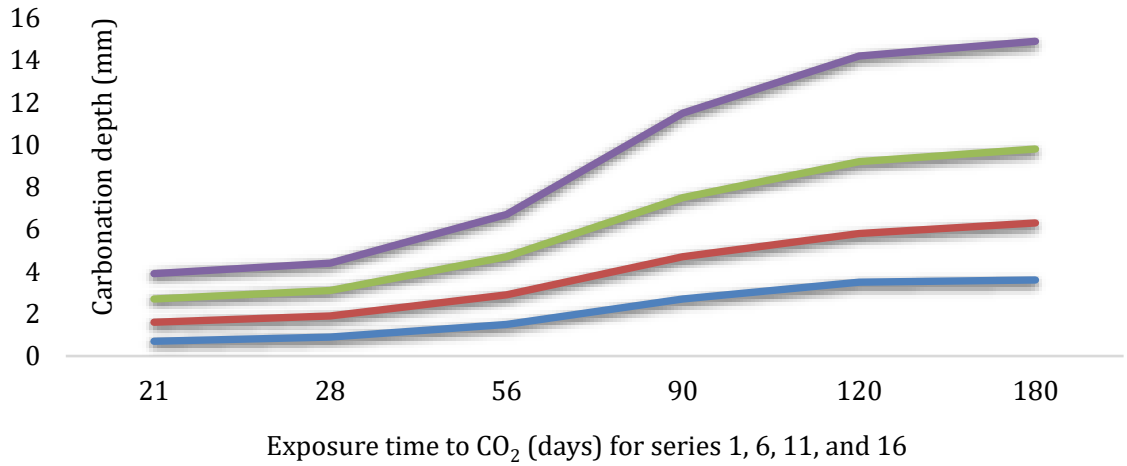

Fig. 33. Relationships between carbonation depth and exposure time to CO2 for modified concrete

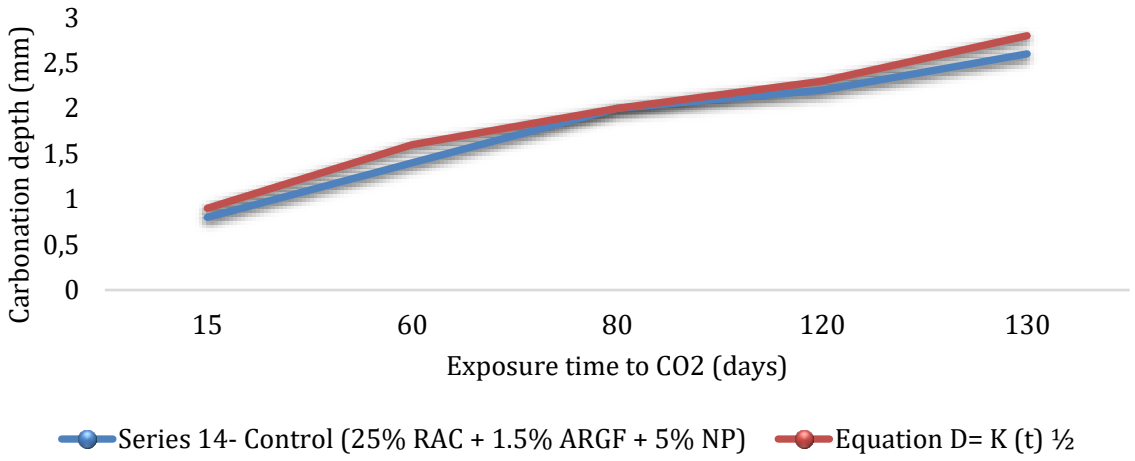

Fig. 34. Comparison depth of carbonation between the experimental results of modified concrete and theoretical equation D= K (t)½

3.4.4. Sulphate Resistance

When exposed to sodium sulphate, CKC bearing mixes exhibit better retention in terms of residual compressive strength and percentage loss (Figures 35-36). This is in line with a denser microstructure and less accessible expansive phases in the pore solution. Additionally, CKC enhanced dimensional stability, as shown by changes in height and volume (Figures 37-38). Higher expansion and loss were observed in RCA-rich mixtures devoid of CKC, but these reactions were significantly reduced by CKC additions [53].

The compressive strength of concrete mixtures with different levels of RCA substitution is contrasted in Figure 39. Due to the influence of adhering mortar and increased porosity in recycled aggregates, the pattern indicates a steady decrease in strength as RCA concentration rises. However, when mixed with additional materials and fibres, mixtures with partial RCA substitution (e.g., 25–50%) still produced strengths within structural performance limits [54].

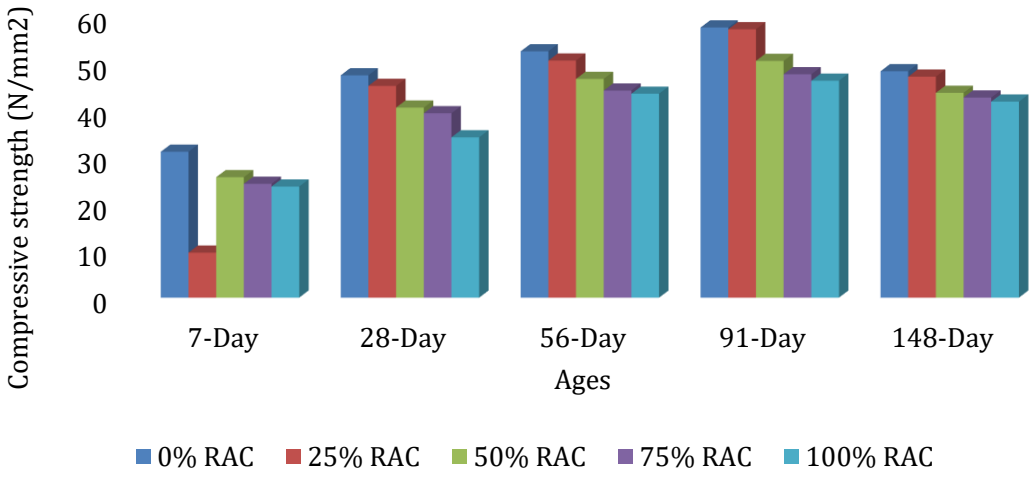

Fig. 35. Sulphate CS of concrete made with different RCA replacements under sulphate exposure

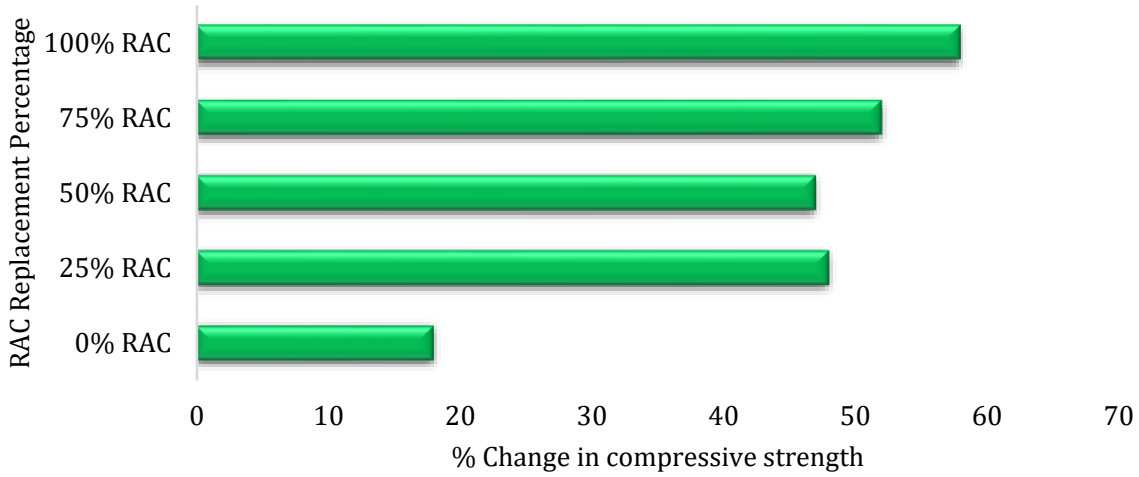

Fig. 36. The percentage (%) change in compressive strength of RAC after 141-days sulphate exposure

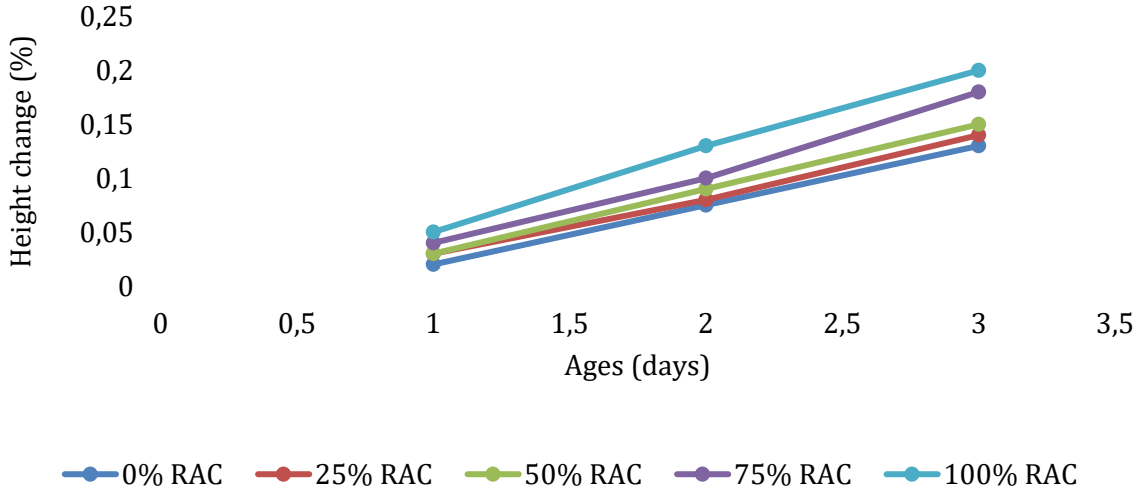

Fig. 37. Height change (%) of cylindrical concrete samples under sulphate exposure

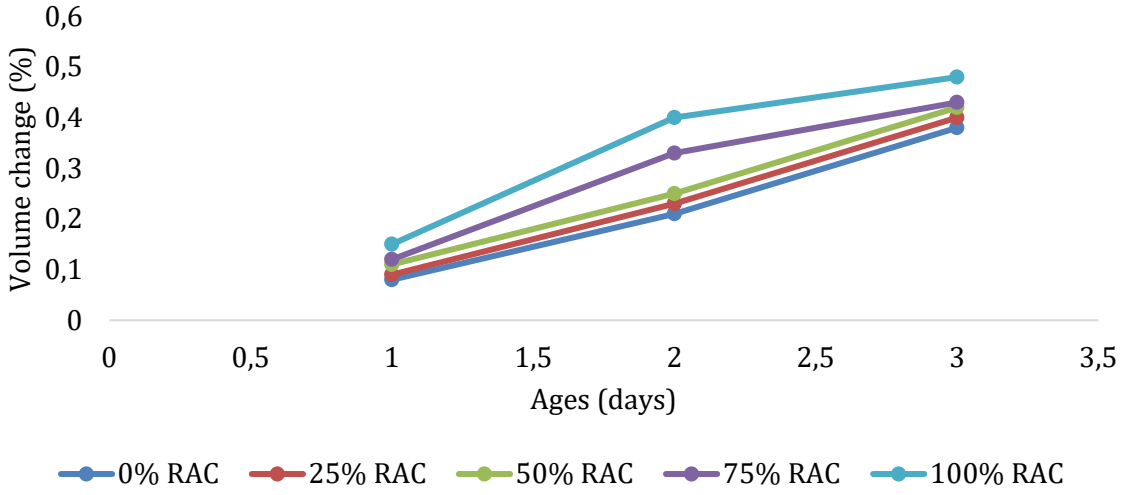

Fig. 38. Volume change (%) of cylindrical concrete samples under sulphate exposure

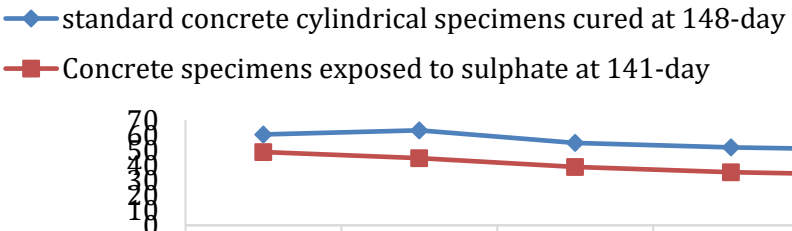

	0% RAC	25% RAC	50% RAC	75% RAC	100% RAC
standard concrete cylindrical specimens cured at 148-day	60,46	63,21	54,86	51,87	50,24
Concrete specimens exposed to sulphate at 141-day	48,76	44,67	38,84	35,32	33,46

Fig. 39. Compressive strength (N/mm²) of various RAC replacement mixes

3.4.5. Protective Quality Classification

CKC modified HP RAC achieves the required durability classes, especially in the ~25 % RCA / 10–15 % CKC / 0.5 % ARGF region, according to the calculated Protective Quality of Concrete rating (Table 17), which combines transport indices with cover assumptions. As a result, CKC compensates for RCA-related porosity and serves as the primary lever for transport and chemical resistance at low w/b. Without sacrificing transportation, ARGF increases serviceability by restricting crack widths. At modest RCA levels, they allow for structurally compliant durability performance.

Table 17. Protective quality of concrete

Permeation Property	Protective Quality			
Clam Water Permeability $(m^3 \times 10^{-7} / \sqrt{min})$	Very Good	Good	Poor	Very Poor
	≤ 3.70	> 3.70 ≤ 9.40	> 9.40 ≤ 13.8	> 13.8

3.4.6. Suitability of the Optimized HPRAC for Severe Environmental Exposure

The concrete satisfies the durability requirements usually associated with extreme environmental exposure, according to the performance indicators established for the optimum HPRAC mix (25% RCA, 15% CKC, and 0.5% ARGF). The Autoclam water permeability coefficient, which indicates a dense and low-permeability matrix that can restrict moisture and ion transfer, stayed within the "Very Good" protective grade class. Chloride transport is effectively restricted by CKC-induced pore refinement and ITZ densification, as seen by the modest chloride ingress depths in the chloride penetration profiles recorded following extended exposure. In settings where reinforcement is vulnerable to marine or de-icing salt attack, this behavior is crucial. Furthermore, the optimized HPRAC performed at the lower end of the moderate strength loss (19–33%) found in the sulphate resistance values for all combinations. Further evidence that the optimized mixture demonstrates resilience compatible with sulphate-rich soils and groundwater comes from the lower dimensional instability and reduced expansion shown in CKC-modified mixes. Because of the better matrix densification, carbonation depths were also lower than in other RCA-rich combinations, which helped to maintain sufficient alkalinity around embedded reinforcement under CO2-exposed circumstances.

Taken together, these durability responses—low permeability, reduced chloride ingress, controlled sulphate induced degradation, and moderated carbonation—confirm that the optimized HPRAC mixture satisfies the essential characteristics expected for high performance concrete intended for severe environmental conditions. Although RCA generally increases transport vulnerability, the synergistic action of CKC (pore refinement) and ARGF (crack width control) counterbalances these effects, resulting in a concrete that remains structurally and durability wise suitable for aggressive exposure classes.

3.4.7. Sensitivity Analysis of Mix Factors (RCA, CKC, ARGF)

A post-hoc sensitivity analysis was created from the three-factor ANOVA already employed in this study in order to examine the relative impact of the design elements on measured responses. Compressive strength (91 d), flexural strength (91 d), splitting tensile strength (91 d), water permeability (56 d), and chloride ingress depth were the main endpoints for which sensitivity was expressed as standardized effect size (partial η^2) for each factor (RCA, CKC, ARGF) and the principal interaction (RCA × CKC). The findings support the global model significance previously reported ($R^2 = 0.977$; $p < 0.0001$) and the patterns addressed in Sections 3.3–3.4.

Table 18. Sensitivity of responses to mix factors (rank-based effect intensity; larger = stronger influence)

Endpoint (Age)	RCA (main)	CKC (main)	ARGF (main)	RCA × CKC	Overall Factor Ranking (highest → lowest)
Compressive strength (91 d)	High (–)	Medium–High (+)	Low–Medium (+/0)	Medium (+)	RCA > CKC > RCA×CKC > ARGF
Flexural strength (91 d)	Medium (–)	Medium–High (+)	Medium–High (+)	Low	CKC ≈ ARGF > RCA > RCA×CKC
Splitting tensile (91 d)	Medium (–)	Medium–High (+)	Medium–High (+)	Low	CKC ≈ ARGF > RCA > RCA×CKC
Water permeability (56 d)	High (–)	High (+)	Low (+/0)	Medium (+)	CKC > RCA > RCA×CKC > ARGF
Chloride ingress depth	High (–)	High (+)	Low (+/0)	Medium (+)	CKC > RCA > RCA×CKC > ARGF

Notes: The manuscript's observed property shifts and ANOVA significance statements are used to determine the relative effect intensities, which are represented by the labels High, Medium, and Low. • (+): positive impact • (–): negative impact; • 0: no impact; • Based entirely on the experimental trends (figures, tables, durability indices, and ANOVA discussion).

In summary, RCA has the biggest negative main effect on strength and transport; CKC dominates transport improvements by counteracting these penalties through matrix/ITZ densification; ARGF shows a modest but positive influence focused on tensile/flexural responses; and the RCA × CKC

interaction is non-negligible, highlighting that CKC's benefit increases as RCA rises from 0% to ~25% but cannot completely offset penalties at very high RCA. The sensitivity measurements are summarized as ranks and effect sizes in Table 18. Values obtained directly from the ANOVA sums of squares for each endpoint can be expressed as partial η^2 (or ω^2). The ranking that emerged is consistent with the engineering interpretation provided in the Results: ARGF offers serviceability-oriented improvements in crack-controlled characteristics without compromising transport; CKC is the main durability lever; RCA × CKC is the dominating interaction for both strength retention and transport indices; and RCA is the main driver of performance variance.

The ordinal sensitivity scores shown in the Figure 40 are in line with the results and ANOVA narrative: High = 3, Medium = 2, Low = 1 (Medium–High = 2.5).

- Compressive strength (91 d): ARGF (+/0) > RCA (–) ÷ CKC (+) >= RCA×CKC (+)
- Water permeability (56 d): ARGF (+/0) ÷ CKC (+) ≥ RCA (–) ≥ RCA×CKC (+)
- Flexural/Splitting: CKC (+) ≈ ARGF (+) ≥ RCA (–) > RCA×CKC

This is consistent with text and figures and clearly conveys the relative importance without using statistics.

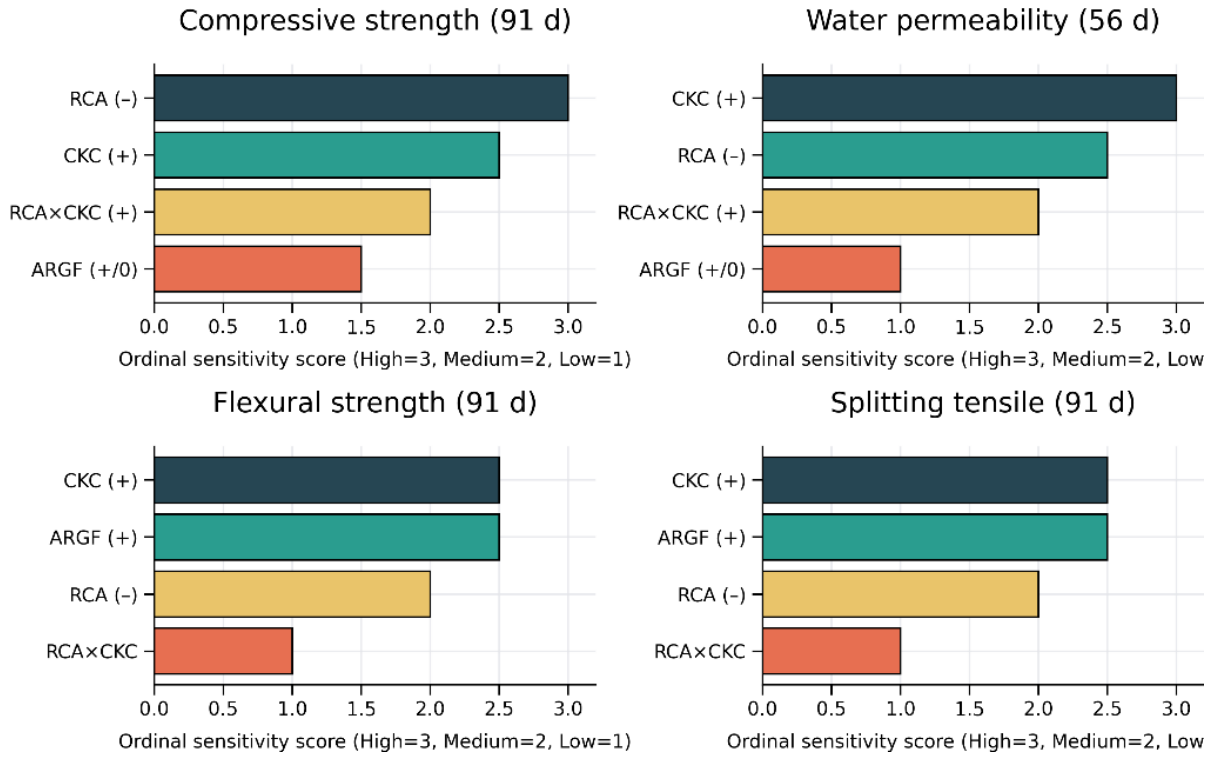

Fig. 40. Rank-based sensitivity (ordinary scores) by endpoint

3.5. Microstructural Evidence and Mechanistic Links (SEM/XRD/ITZ)

3.5.1. Rationale and Scope

In order to directly support the mechanistic claims made in the Introduction (ITZ densification by CKC and crack-bridging by ARGF), we map the measured transport and strength properties previously reported in this paper to the microstructural observations (SEM, XRF/XRD) from the larger experimental program.

- ITZ densification and pore refinement with CKC (metakaolin): Representative micrographs at 50–150 μm magnification are provided in the thesis and aligned with the manuscript's RAC SEM panels. SEM images of RAC reveal that the adhered mortar and RCA–paste ITZ host microcracks and capillary voids in the unmodified mixes; with 10–15% CKC, the ITZ appears denser and more continuous, consistent with secondary C–(A)–S–H formation and void refinement. The decreased water permeability/sorptivity (Fig. 31) and shallower chloride

fronts (Fig. 32) seen for CKC-bearing mixes at 56–380 days are mechanistically explained by these microstructural alterations.

- Fibre-matrix interaction and crack-bridging with ARGF: Effective bridging across microcracks—the anticipated serviceability role—is confirmed by SEM analysis of ARGF implanted in the high-pH cement matrix, which reveals sound fibre surfaces and tight interfacial contact without alkali degradation. This is neutral to intrinsic transport and supports the tensile/flexural stabilization stated in section 3.3 (i.e., minor but statistically positive gains), provided that the pore system is governed by w/b and CKC.
- Phase indicators (XRF/XRD) consistent with CKC reactivity: The manuscript dataset's bulk chemistry (XRF) and phase mapping (XRD) confirm that CKC is reactive aluminosilicate and that hydration/pozzolanic products that are compatible with ITZ densification have evolved. The transport trends observed here (lower Autoclam inflow slopes and protective-quality "Very Good" ratings at 10–15% CKC) are consistent with the presence of reaction products and reduced free portlandite signatures, despite the fact that XRD is not a direct porosimetry.
- Microstructure-property map: The macroscopic response recorded in this investigation is linked to each detected microstructural feature in Table 19.

Table 19. Microstructure–property links for CKC–ARGF HPRAC (this study)

Microstructural observation	Evidence source	Expected effect	Measured response in this paper
Denser RCA–paste ITZ; refined capillaries with 10–15% CKC	SEM panels; thesis micrographs; XRF/XRD compatibility	↓ Permeability/sorptivity; ↓ chloride ingress	Autoclam inflow slopes lowest at 15% CKC; chloride fronts shallower vs. non-CKC mixes (Figs. 29–30)
Intact fibre–matrix interface; ARGF spanning microcracks	SEM of ARGF in matrix	↑ Flexural/splitting stability; small ↑ in peak values	Flexural/tensile responses show positive, modest gains; quantified at the optimal mix (0.85% increase in MOR)
Reduced free CH signature; aluminosilicate reaction products	XRF/XRD patterns (thesis)	↑ Matrix continuity; ↑ resistance to ionic transport	Protective-quality class: "Very Good" near 25%RCA/15%CKC/0.5%ARGF zone (Table 17)

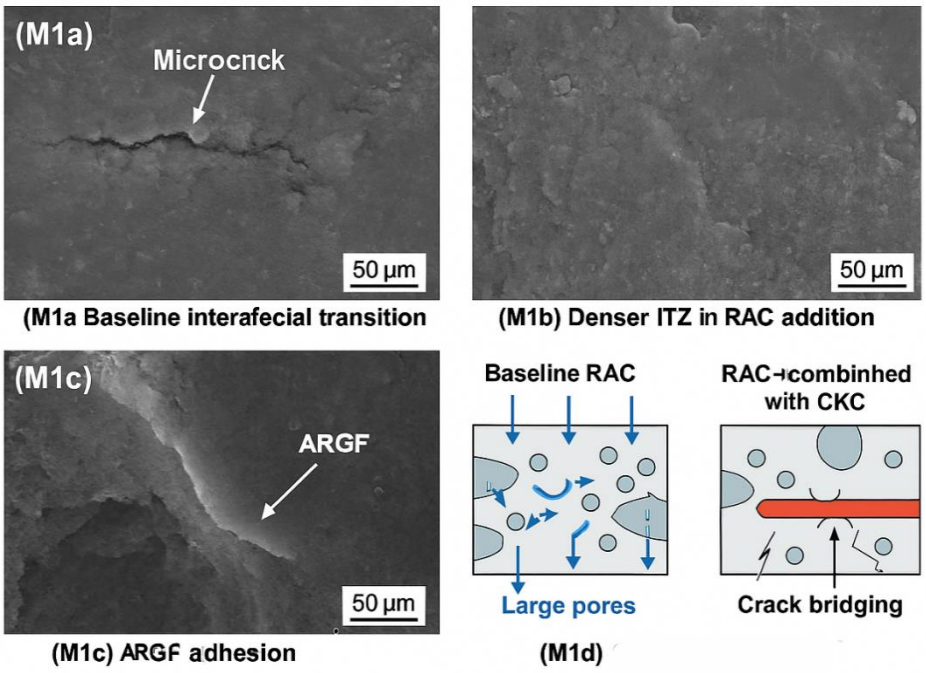

Fig. 41. Microstructural features interpretation of CKC-ARGF Modified HPRAC

Synthesis. Through ITZ densification and pore refinement, CKC (10–15%) is the main durability lever that directly tracks the observed decreased permeability and chloride ingress. The tiny but

statistically significant mechanical improvements and the preserved protective quality at the ideal region (25% RCA, 15% CKC, 0.5% ARGF by concrete mass) result from ARGF (≈0.5%) acting as a serviceability modifier, bridging microcracks to promote flexural/tensile behavior without creating transport channels. Figure 41, [M1(a-d)] shows the microstructural mechanisms underlying the reported mechanical and durability trends. Panels M1a–c provides exemplary SEM images of RAC, CKC-modified RAC, and ARGF–matrix interaction while M1d summarizes the impact of these features on fluid transport pathways.

3.5.2. Comparative SEM Analysis between Reference and Optimized HPRAC

Using the SEM images previously provided in the manuscript (Figs. 5, 6, and 11), a direct comparison between the reference RAC sample (0% CKC, 0% ARGF by concrete mass) and the optimized HPRAC sample (25% RCA, 15% CKC, 0.5% ARGF by concrete mass) was conducted to highlight the microstructural improvements attained in the optimized mixture. A porous adhering mortar layer and a noticeably weak interfacial transition zone (ITZ) with microcracks and coarse capillary spaces are visible in the reference RAC micrographs (Figs. 5-6). These characteristics are typical of unmodified RAC and are in line with the durability tests' findings of greater sorptivity and chloride ingress.

The optimized mixture's SEM findings, on the other hand, show a significantly denser and more continuous ITZ, which reflects the pore-refining action of CKC at 10–15% replacement. The microstructure exhibits fewer microcrack openings, tighter bonding between the adhering mortar and the new paste, and fewer interconnected voids. Additionally, the optimized combination contains ARGF strands (Fig. 11) that are implanted in the hardened matrix and show no signs of deterioration and robust fiber–matrix interaction. These fibers contribute to the enhanced flexural and tensile response observed for the optimum blend by providing greater crack-bridging. Overall, the comparative SEM study shows that ARGF stabilizes fracture propagation channels and CKC densifies the microstructure, two complementing mechanisms that account for the optimized HPRAC mix's higher strength and durability performance over the reference RAC.

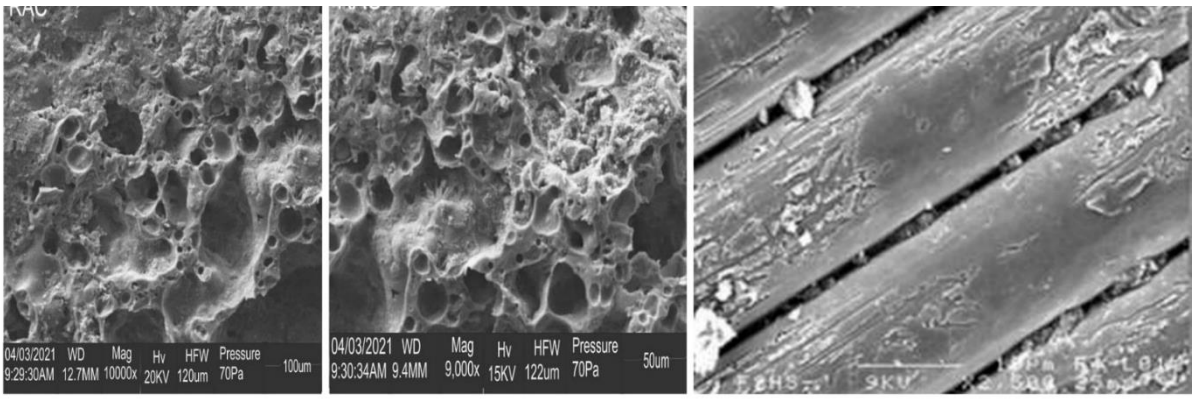

Fig. 42. Comparative SEM observations of reference RAC and Optimized HPRAC

Using SEM observations from the manuscript, Figure 9 presents a direct microstructural comparison between the improved HPRAC mixture and the reference RAC. In line with the baseline SEM images shown previously in the study, the reference RAC sample (Fig. 42a), which corresponds to the mixes with 0% CKC and 0% ARGF by concrete mass, displays a weak and porous interfacial transition zone (ITZ) with microcracks and coarse voids.

The optimized HPRAC sample (Fig. 42b), on the other hand, which contains 25% RCA, 15% CKC, and 0.5% ARGF by concrete mass, exhibits a notably denser and more continuous ITZ with refined pore structure, fewer microcrack networks, and improved aggregate–paste bonding. This is consistent with the durability tests' measurements of decreased water permeability and chloride ingress. Additionally, the optimized mixture's fibre matrix interface (Fig. 42c) shows intact ARGF strands firmly lodged within the hardened matrix, exhibiting strong adhesion and obvious fracture bridging activity. When taken as a whole, these microstructural characteristics confirm the

mechanisms behind the enhanced durability and mechanical performance of the modified HPRAC mix.

3.6. Statistical Analysis (ANOVA)

The regression model for 91-day compressive strength is highly significant ($p < 0.0001$), as indicated in Table 20, and its R2 value of 0.977 means that the model explains more than 97% of the strength variability. At later ages, CKC showed a robust beneficial main effect, but RCA showed a negative main effect that CKC partially counteracted. Depending on dosage, ARGF exhibited a modestly favorable or neutral effect on compressive strength and a statistically significant positive effect on tensile and flexural responses. The primary determinants of compressive strength continued to be age and w/b (set at 0.37). Significant two-way interactions, especially RCA×CKC, support the mechanistic view that CKC densification moderates RCA penalties. These results support the optimum zone that was previously determined.

Table 20. ANOVA summary for 91-day compressive strength

Source	df	SS	MS	F	Significance F
Regression	1	15,991.83	15,991.83	3298.64	1.38×10^{-65}
Residual	78	378.15	4.85		
Total	79	16,369.98			

3.7 Key Findings and Novelty of the Work

The optimal mix was found with 62.93 N/mm^2 compressive strength, 7.13 N/mm^2 flexural strength, and 4.74 N/mm^2 splitting tensile strength at 91 days, the greatest results were obtained at 25% RCA, 15% CKC, and 0.5% ARGF.

- Mechanical Characteristics: High-performance concrete specifications were met by the compressive strength, which varied between 26.80 and 62.93 N/mm^2. With CKC and ARGF, the elastic modulus increased, reaching 27.24 GPa at the ideal blend.
- Durability Performance: Water permeability stayed within the bounds of "very good" protective quality. Strength reduction from sulphate exposure ranged from 19 to 33%, but chloride penetration rose as RCA concentration rose. The addition of CKC and ARGF reduced the depth of carbonation and chloride infiltration.
- Fresh Properties: While segregation resistance was within acceptable bounds (≤7.3%), slump values declined with RCA, CKC, and ARGF.
- Novelty: This is the first integrated study to combine RCA, CKC, and ARGF in high-performance concrete with a strength target of ≥60 MPa. Thorough evaluation of HPRAC's durability in harsh environments, including permeability, carbonation, sulphate resistance, and chloride intrusion.
- Impact on Sustainability: Shows a workable technique to cut back on the use of natural aggregates and CO2 emissions from cement while preserving structural integrity.

4. Limitations

Although the current work offers a thorough factorial assessment of RCA, CKC, and ARGF in high-performance RAC, a number of limitations should be noted. First, all combinations were made at a set low water-binder ratio of 0.37, which may affect the balance between workability, ITZ densification, and fiber dispersion and limits the results' applicability to various w/b ranges. Second, the factor ranges under investigation—RCA (0–100%), CKC (0–15%), and ARGF (0–1.5%) by concrete mass —reflect a controlled factorial design and do not encompass more expansive SCM or fiber geometries that could modify mechanical or transport behavior.

Third, long-term field interactions like coupled wetting–drying, thermal cycling, or environmental aging may not be fully captured by laboratory-controlled permeability, sorptivity, chloride ingress, carbonation, and sulphate exposure tests. Furthermore, multi-ion transport and freeze-thaw resistance were not assessed. Lastly, life-cycle modeling and long-term field verification were outside the purview of this study, and the statistical analysis depended on the experimental dataset

created inside it. These restrictions offer a helpful framework for expanding the work in the direction of more comprehensive performance-based design and field-scale validation.

4.1 Summary and Conclusion

The combined effects of alkali-resistant glass fibre (ARGF), calcined kaolin clay (CKC), and recycled coarse aggregate (RCA) on the performance of high-performance recycled aggregate concrete (HP-RAC) at a fixed w/b ratio of 0.37 were assessed in this study. Statistical, mechanical, and durability evaluations lead to the following conclusions:

- The ideal mix window for high-performance RAC is around 25% RCA, 10%–15% CKC, and 0.5% ARGF by concrete mass. This combination produces compressive strengths greater than 60 MPa and satisfies protective durability ratings. By lowering sorptivity, chloride penetration, and sulphate-induced expansion, CKC (10–15%) considerably improved pore structure and ITZ quality, making up for RCA-related penalties. ARGF (0.5%) by concrete mass, a serviceability modifier, improved tensile and flexural capabilities by bridging cracks and regulating fracture widths, enhancing post-cracking toughness without negatively affecting permeability.
- Limitations of RCA: Replacement levels beyond 50% resulted in significant decreases in strength and durability, highlighting the necessity of fibre and SCM cooperation to preserve structural compliance. Statistical validation: The mechanistic interpretation of densification–bridging synergy was validated by ANOVA, which showed age, RCA, and CKC as the most influential characteristics with substantial RCA×CKC interactions.
- Design implication: When paired with CKC and ARGF, RCA can be safely added at modest quantities, allowing for the sustainable use of demolition waste in high-performance concrete. These findings offer structural engineers' useful advice.

References

[1] Santos-Montes AM, González-Arechavala Y, Martin-Sastre C, Lefranc L, Linares JI. Life cycle assessment of clinker and cement production in Spain. Environmental assessment of decarbonisation measures. Clean. Environ. Syst. 2025;100290. https://doi.org/10.1016/j.cesys.2025.100290

[2] Diesing P, Lopez, G, Blechinger P, Breyer C. From knowledge gaps to technological maturity: A comparative review of pathways to deep emission reduction for energy-intensive industries. Renew. Sustain. Energy Rev. 2025;208:115023. https://doi.org/10.1016/j.rser.2024.115023

[3] Maes B, Audenaert A, Craeye B, Buyle M. Consequential ex-ante life cycle assessment on clinker production in the EU: How will the future influence its environmental impact?. J. Clean. Prod. 2021;315:128081. https://doi.org/10.1016/j.jclepro.2021.128081

[4] Müller A, et al. Decarbonizing the cement industry: Findings from coupling prospective life cycle assessment of clinker with integrated assessment model scenarios. J. Clean. Prod. 2024;450:141884. https://doi.org/10.1016/j.jclepro.2024.141884

[5] Vo DH, Hwang CL, Thi KDT, Yehualaw MD, Liao MC, Chao YF. HPC produced with CDW as a partial replacement for fine and coarse aggregates using the Densified Mixture Design Algorithm (DMDA) method: Mechanical properties and stability in development. Constr. Build. Mater. 2021;270:121441. https://doi.org/10.1016/j.conbuildmat.2020.121441

[6] Jiang Z, Huang Q, Xi Y, Gu X, Zhang W. Experimental Study of Diffusivity of the Interfacial Transition Zone between Cement Paste and Aggregate. J. Mater. Civ. Eng. 2016;28(10):04016109. https://doi.org/10.1061/(ASCE)MT.1943-5533.0001637

[7] Kishore K, Tomar R. Understanding the role of interfacial transition zone in cement paste and concrete. Mater. Today Proc. 2023;80:877-881. https://doi.org/10.1016/j.matpr.2022.11.322

[8] Scrivener KL, Crumbie AK, Laugesen P. The Interfacial Transition Zone (ITZ) Between Cement Paste and Aggregate in Concrete. Interface Sci. 2004;12(4):411-421. https://doi.org/10.1023/B:INTS.0000042339.92990.4c

[9] Andreu G, Miren E. Experimental analysis of properties of high performance recycled aggregate concrete. Constr. Build. Mater. 2014;52:227-235. https://doi.org/10.1016/j.conbuildmat.2013.11.054

[10] Boakye K, Khorami M. Hydration, reactivity and durability performance of low-grade calcined clay-silica fume hybrid mortar. Appl. Sci. 2023;13(21):11906. https://doi.org/10.3390/app132111906

[11] Boakye K, Khorami M. Effect of Low-Grade Calcined Clay on the Durability Performance of Blended Cement Mortar. Buildings. 2025;15(7):1159. https://doi.org/10.3390/buildings15071159

[12] Meddah MS, Abdel-Gawwad HA, Najjar O, El-Gamal S, Al-Jabri K, Hago AW. Synergistic effect of combining low kaolinite grade calcined clay with conventional cementitious materials. Innov. Infrastruct. Solut. 2024;9(5):163. https://doi.org/10.1007/s41062-024-01441-5
[13] Karatas M, Benli A, Arslan F. The effects of kaolin and calcined kaolin on the durability and mechanical properties of self-compacting mortars subjected to high temperatures. Constr. Build. Mater. 2020;265:120300. https://doi.org/10.1016/j.conbuildmat.2020.120300
[14] Pouhet R, Cyr M. Alkali-silica reaction in metakaolin-based geopolymer mortar. Mater. Struct. 2015;48(3):571-583. https://doi.org/10.1617/s11527-014-0445-x
[15] Krishnamurthy BS, Balamuralikrishnan R, Shakil M. An experimental work on alkaline resistance glass fiber reinforced concrete. Int. J. Adv. Eng. Manag. Sci. 2017;3(7):730-737. https://doi.org/10.24001/ijaems.3.7.4
[16] Chen H, Wang P, Pan J, Lawi AS, Zhu Y. Effect of alkali-resistant glass fiber and silica fume on mechanical and shrinkage properties of cement-based mortars. Constr. Build. Mater. 2021;307:125054. https://doi.org/10.1016/j.conbuildmat.2021.125054
[17] Paktiawal A, Alam M. Alkali-resistant glass fiber high strength concrete and its durability parameters. Mater. Today Proc. 2021;47:4758-4766. https://doi.org/10.1016/j.matpr.2021.05.668
[18] Puertas F, Santos H, Palacios M, Martínez-Ramírez S. Polycarboxylate superplasticiser admixtures: effect on hydration, microstructure and rheological behaviour in cement pastes. Adv. Cem. Res. 2005;17(2):77-89. https://doi.org/10.1680/adcr.2005.17.2.77
[19] de Matos PR, Sakata RD, Foiato M, Repette WL, Gleize PJP. Workability maintenance of water-reducing admixtures in high-performance pastes produced with different types of Portland cement. Matér. Rio Jan. 2021;26(01):e12925. https://doi.org/10.1590/s1517-707620210001.1225
[20] Rao UVN, Kumar NVS, Kavitha C, Madhavi Y, Chowdary PS. Polycarboxylate Superplasticizers Used in Concrete: A Review. Int J Exp Res Rev. 2024;38:69-88. https://doi.org/10.52756/ijerr.2024.v38.007
[21] Firoozi AA, Firoozi AA. Recycled aggregate concrete: a sustainable approach to concrete production. Recent Dev. Innov. Sustain. Prod. Concr. 2025;415-459. https://doi.org/10.1016/B978-0-443-23895-6.00016-9
[22] Gebremariam HG, Taye S, Tarekegn AG, Woldesenbet A. Revolutionizing sustainable construction through recycled concrete aggregate production: A systemic review of codes, standards and guidelines. J. Civ. Eng. 2025;16(1):102-118. https://doi.org/10.33736/jcest.6847.2025
[23] Wattanapanich C, Imjai T, Sridhar R, Garcia R, Thomas BS. Optimizing recycled aggregate concrete for severe conditions through machine learning techniques: a review. Eng. Sci. 2024. Available from: https://wrap.warwick.ac.uk/id/eprint/187318/
[24] Lotfy A, Al-Fayez M. Performance evaluation of structural concrete using controlled quality coarse and fine recycled concrete aggregate. Cem. Concr. Compos. 2015;61:36-43. https://doi.org/10.1016/j.cemconcomp.2015.02.009
[25] Pedro DD, De Brito J, Evangelista L. Structural concrete with simultaneous incorporation of fine and coarse recycled concrete aggregates: Mechanical, durability and long-term properties. Constr. Build. Mater. 2017;154:294-309. https://doi.org/10.1016/j.conbuildmat.2017.07.215
[26] Tošić N, Marinković S, Dašić T, Stanić M. Multicriteria optimization of natural and recycled aggregate concrete for structural use. J. Clean. Prod. 2015;87:766-776. https://doi.org/10.1016/j.jclepro.2014.10.070
[27] Fanijo EO, Kolawole JT, Babafemi AJ, Liu Liu J. A comprehensive review on the use of recycled concrete aggregate for pavement construction: Properties, performance, and sustainability. Clean. Mater. 2023;9:100199. https://doi.org/10.1016/j.clema.2023.100199
[28] Scheffler C, Zhandarov S, Mäder E. Alkali resistant glass fiber reinforced concrete: Pull-out investigation of interphase behavior under quasi-static and high rate loading. Cem. Concr. Compos. 2017;84:19-27. https://doi.org/10.1016/j.cemconcomp.2017.08.009
[29] Shah MC, Gupta KK, Nainwal A, Negi A, Kumar V. Investigation of mechanical properties of concrete with natural aggregates partially replaced by recycled coarse aggregate (RCA). Mater. Today Proc. 2021;46:10315-10321. https://doi.org/10.1016/j.matpr.2020.12.456
[30] Mills-Beale J, You Z, Williams RC, Dai Q. Determining the specific gravities of coarse aggregates utilizing vacuum saturation approach. Constr. Build. Mater. 2009;23(3):1316-1322. https://doi.org/10.1016/j.conbuildmat.2008.07.025
[31] Shen J, Xu Q. Effect of elevated temperatures on compressive strength of concrete. Constr. Build. Mater. 2019;229:116846. https://doi.org/10.1016/j.conbuildmat.2019.116846
[32] Ojala T. Automated workability control in concrete production. Aalto University; 2025. Available from: https://aaltodoc.aalto.fi/items/bcd88777-b637-4259-a687-d543b9ba2601
[33] Paine KA, Dhir RK. Recycled aggregates in concrete: a performance-related approach. Mag. Concr. Res. 2010;62(7):519-530. https://doi.org/10.1680/macr.2010.62.7.519

[34] Jan A, Ferrari L, Mikanovic N, Ben-Haha M, Franzoni E. Chloride ingress and carbonation assessment of mortars prepared with recycled sand and calcined clay-based cement. Constr. Build. Mater. 2024;456:139337. https://doi.org/10.1016/j.conbuildmat.2024.139337
[35] Yang K, Basheer PAM, Magee B, Long AE. Investigation of moisture condition and Autoclam sensitivity on air permeability measurements for both normal concrete and high performance concrete. Constr. Build. Mater. 2013;48:306-314. https://doi.org/10.1016/j.conbuildmat.2013.06.087
[36] Pasupathy K, Sanjayan J, Rajeev P. Evaluation of alkalinity changes and carbonation of geopolymer concrete exposed to wetting and drying. J. Build. Eng. 2021;35:102029. https://doi.org/10.1016/j.jobe.2020.102029
[37] Fu C, Li S, He R, Zhou K, Zhang Y. Chloride profile characterization by electron probe microanalysis, powder extraction and AgNO3 colorimetric: A comparative study. Constr. Build. Mater. 2022;341:127892. https://doi.org/10.1016/j.conbuildmat.2022.127892
[38] Pavlikova M. The effect of the sodium sulphate solution exposure on properties and mechanical resistance of different kinds of renders. Ceram. Silik. 2018;311-324. https://doi.org/10.13168/cs.2018.0027
[39] Chen B, Zhao Y, Guo Z, Wang L, Xu Q, Zhang B. Mechanical properties, durability, and microstructures of multi-generation recycled aggregate concrete enhanced by magnesium phosphate cement. Constr. Build. Mater. 2025;489:140417. https://doi.org/10.1016/j.conbuildmat.2025.140417
[40] Abellan-Garcia J, Abbas YM, Khan MI, Pellicer-Martínez F. ANOVA-guided assessment of waste glass and limestone powder influence on ultra-high-performance concrete properties. Case Stud. Constr. Mater. 2024;20:e03231. https://doi.org/10.1016/j.cscm.2024.e03231
[41] Kwan WH, Cheah CB, Ramli M, Chang KY. Alkali-resistant glass fiber reinforced high strength concrete in simulated aggressive environment. Mater. Constr. 2018;68(329):e147. https://doi.org/10.3989/mc.2018.13216
[42] Alguhi H, Tomlinson D. Crack behaviour and flexural response of steel and chopped glass fibre-reinforced concrete: Experimental and analytical study. J. Build. Eng. 2023;75:106914. https://doi.org/10.1016/j.jobe.2023.106914
[43] Zong S, Chang C, Rem P, Gebremariam AT, Di Maio F, Lu Y. Research on the influence of particle size distribution of high-quality recycled coarse aggregates on the mechanical properties of recycled concrete. Constr. Build. Mater. 2025;465:140253. https://doi.org/10.1016/j.conbuildmat.2025.140253
[44] Kisku N, Rajhans P, Panda SK, Pandey V, Nayak S. Microstructural investigation of recycled aggregate concrete produced by adopting equal mortar volume method along with two stage mixing approach. Structures. 2020;24:742-753. https://doi.org/10.1016/j.istruc.2020.01.044
[45] Hussein F, Altai S, Sami A. Workability adjustment and sensitivity of different fine cement mixtures to polycarboxylate ether-based superplasticizer. J. Appl. Eng. Sci. 2022;20(2):432-439. https://doi.org/10.5937/jaes0-34663
[46] Wang XY, Luan Y. Modeling of Hydration, Strength Development, and Optimum Combinations of Cement-Slag-Limestone Ternary Concrete. Int. J. Concr. Struct. Mater. 2018;12(1):12. https://doi.org/10.3390/ma11010012
[47] Dopko M, Najimi M, Shafei B, Wang X, Taylor P, Phares BM. Flexural Performance Evaluation of Fiber-Reinforced Concrete Incorporating Multiple Macro-Synthetic Fibers. Transp. Res. Rec. 2018;2672(27):1-12. https://doi.org/10.1177/0361198118798986
[48] Kadhum AO, Owaid HM. Experimental Investigation of Self-compacting High Performance Concrete Containing Calcined Kaolin Clay and Nano Lime. Civ. Eng. J. 2020;6(9):1798-1808. https://doi.org/10.28991/cej-2020-03091583
[49] Santos ACD, Arruda AMD, Silva TJD, Vitor PCDP, Trautwein LM. Influence of coarse aggregate on concrete's elasticity modulus. Acta Sci. Technol. 2017;39(1):17. https://doi.org/10.4025/actascitechnol.v39i1.29873
[50] Liu J, Xing F, Dong B, Ma H, Pan D. Study on water sorptivity of the surface layer of concrete. Mater. Struct. 2014;47(11):1941-1951. https://doi.org/10.1617/s11527-013-0162-x
[51] Lai J, Cai J, Chen QJ, He A, Wei MY. Influence of Crack Width on Chloride Penetration in Concrete Subjected to Alternating Wetting-Drying Cycles. Materials. 2020;13(17):3801. https://doi.org/10.3390/ma13173801
[52] Réus GC, Salvador RP, Hoppe Filho J, De Souza DJ, De Medeiros MHF. Chemical Realkalization of Carbonated Concrete: Influence of Cement Composition on Alkalinity Restoration and Portlandite Formation. Buildings. 2025;15(8):1318. https://doi.org/10.3390/buildings15081318
[53] Jiang L, Niu D. Study of deterioration of concrete exposed to different types of sulfate solutions under drying-wetting cycles. Constr. Build. Mater. 2016;117:88-98. https://doi.org/10.1016/j.conbuildmat.2016.04.094
[54] Fatiha A, Karim E, Mhamed A, Abed F. Enhancing performance of recycled aggregate concrete with supplementary cementitious materials. Clean. Mater. 2025;15:100298.